universität
wien

MASTERARBEIT

Titel der Masterarbeit

"Mechanism of Ras protein transfer from tumor cells to endothelial cells"

verfasst von

Markus Peter Maximilian Kraller, BSc

angestrebter akademischer Grad

Master of Science (MSc)

Wien, 2014

DANKSAGUNG

TABLE OF CONTENTS

1. INTRODUCTION

1.1 Ras proteins

1.1.1 The Ras family – synthesis, modification and trafficking

Studying two cancer-causing viruses, the Harvey sarcoma virus and Kirsten sarcoma virus, two out of three homologous human Ras genes could be identified by Scolnick, Chang and colleagues at the National Institutes of Health [1]. According to the names of the viruses the genes were named *H-Ras* and *K-Ras* [2]. The third Ras gene was identified in human neuroblastoma cells and therefore called *N-Ras* [3]. These three Ras proto-oncogenes encode four protein isoforms: H-Ras, K-Ras4A, K-Ras4B and N-Ras [2]. All of them are ubiquitously expressed in various cell types but in different amounts. Even though it is not entirely resolved, several studies point to isoform specific signaling ranging from receptor tyrosine kinase activation at the cell surface in the case of H-Ras or K-Ras to signaling from endomembrane compartments including N-Ras [4-5]. All of the Ras proteins belong to the superfamily of small GTPases and function as a molecular switch that can trigger signaling cascades. They can be compared to the α-subunit of heterotrimeric G proteins in biochemistry and function, but they function as a monomer [6]. Focusing on the amino acid composition of all four Ras isoforms there is almost a complete sequence homology in the first 185 amino acids containing all important nucleotide binding and effector domains [2, 6]. The first 185 amino acids are followed by the so called "hypervariable region (HVR)" which is a short 23-24 amino acid stretch at the C-terminus of the Ras molecule and it is the only area where a significant sequence divergence can be observed. This divergence determines the different isoforms (Fig. 1) [7]. The HVR is subjected to several post-translational modifications that lead to different membrane localizations and it is terminated by a characteristic four amino acid long CaaX motif which is the target of post-translational modifications [8]. Ras proteins synthesized in the cytosol are farnesylated on the cysteine of the CaaX motif by farnesyl protein transferase [8]. This first post-translational modification leads to attachment to the endoplasmatic reticulum (ER). Ras-converting enzyme 1 (Rce1; homologous to Afc1p/Ste24p and Rce1p in yeast) which is located at the ER cleaves the aaX off the farnesylated CaaX motif and the cysteine is then carboxymethylated by the isoprenyl cysteine methyl transferase (Icmt; homologous to Ste14p in yeast) [9-10]. C-terminal farnesylation of the Ras proteins only leads to a weak membrane binding capacity and is further strengthened by a second modification which varies among the Ras isoforms. H-, N- and the 4A splice

variant of K-Ras (K-Ras4A) undergo palmitoylation on one or two cysteines of the HVR. In contrast, the 4B splice variant of K-Ras (K-Ras4B) contains a hexa-lysine polybasic sequence that leads to a strong interaction between its positively charged lysine residues and the negatively charged lipid head groups of the membrane [11]. As K(A)-Ras and N-Ras are only monopalmitoylated there is a third motif in the HVR consisting of basic/hydrophobic amino acids that lead to a better plasma membrane binding [7]. After the steps of post-translational modification H-Ras, K-Ras4A and N-Ras are transported to the plasma membrane via the conventional secretory pathway. However, the K-Ras4B isoform is transported to the plasma membrane via a Golgi-independent pathway that involves mitochondrial function and class C vps proteins [12-14]. At the plasma membrane the HVR motifs are responsible for interactions with different microdomains (Fig. 2). Of note, all Ras isoforms are known to shuttle between the plasma membrane and intracellular compartments which also seems to support the signaling process [15].

Fig. 1: Hypervariable region (HVR) of the four Ras isoforms:

A distinct composition of the C-terminal HVR of the four Ras isoforms leads to different post-translational lipid modifications. These result in different trafficking pathways and plasma membrane localizations. All four isoforms contain the C-terminal CaaX motif in which the cysteine is farnesylated. This results in attachment to the ER. Next the aaX sequence is cleaved off and the cysteine is carboxymethylated. Thereafter, H-, N- and K(A)-Ras undergo palmitoylation on one or two cysteines of the HVR to strengthen the membrane binding capacity. In contrast, K(B)-Ras contains a hexa-lysine polybasic sequence that is responsible for membrane anchoring by interaction with the negatively charged lipid head groups of the membrane. Figure adapted from [7].
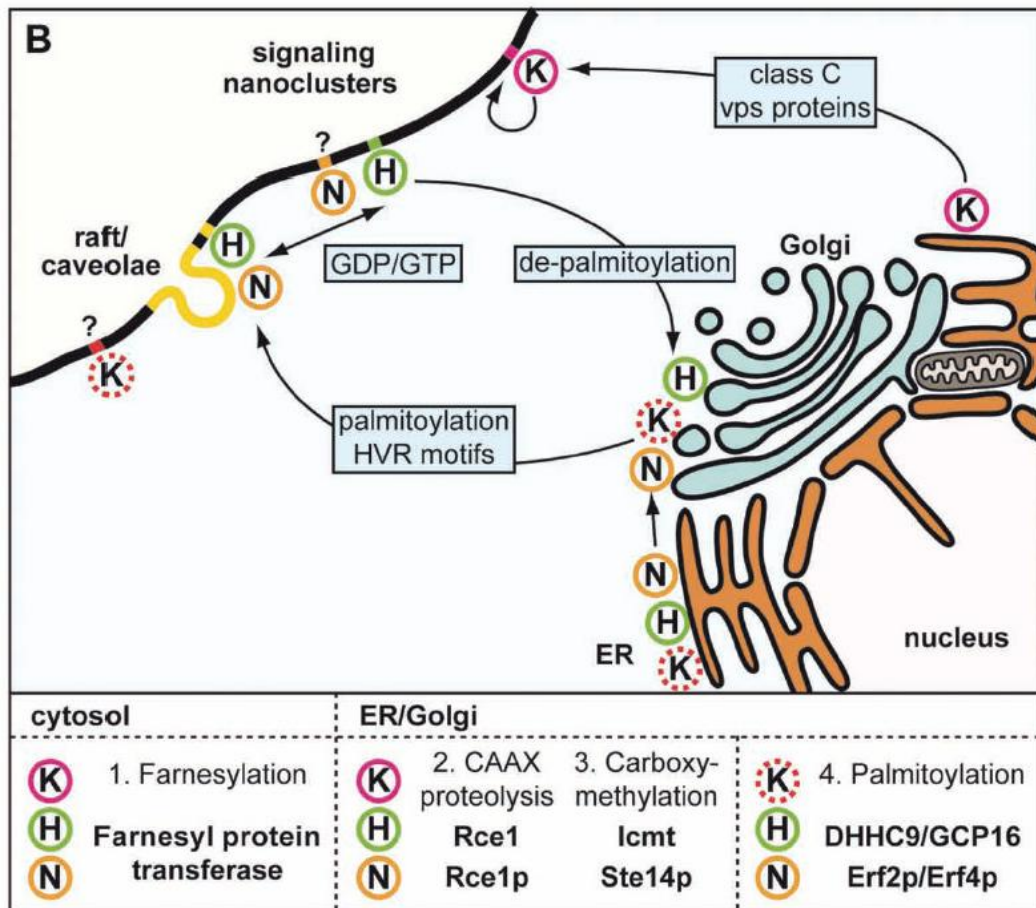
Fig. 2: Different trafficking routes and locations in the plasma membrane of the Ras isoforms:

After post-translational modification H-Ras, K-Ras4A and N-Ras are transported from the ER to the Golgi apparatus. From this point they are integrated in the conventional secretory pathway and delivered to the plasma membrane where they cluster in raft domains depending on their activation state. K-Ras4B does not follow this pathway and it is proposed that class C vps proteins are responsible for the transport to the plasma membrane. Moreover K-Ras4B is located in membrane domains distinct from H-Ras and N-Ras which may promote different functions of the isoforms. Figure adapted from [7].

1.1.2 Ras proteins – small GTPases

Like other small GTPases membrane-bound Ras is activated via ligand - receptor interaction [4]. A ligand such as epidermal growth factor (EGF) which binds to its receptor tyrosine kinase (EGFR or HER2) leads to dimerization and autophosphorylation of the receptor cytoplasmic domain (Fig. 3). This first step of activation is followed by recruitment of phosphotyrosine-binding adaptor molecules such as Shc (Src homology 2 domain containing) protein and Grb2 (growth factor receptor-bound protein 2) [16]. Both, Shc and Grb2 contain SH2 (Src homology 2) domains which allow binding to phosphorylated tyrosine residues [17]. Shc and Grb2 further bind the guanine nucleotide exchange factor (GEF) son of sevenless (SOS). SOS is capable of interacting with inactivated GDP-bound Ras and forcing the Ras molecule to release the bound GDP. Upon GDP release the Ras molecule quickly

binds GTP, which is generally more abundant in the cytoplasm, and is thereby transformed into its active GTP-bound state. Thereafter, GTP-Ras can activate several downstream interaction partners resulting in cell proliferation, differentiation, migration, survival or apoptosis [2, 16]. The best described factors are Raf kinases, the phosphatidylinositol-3-kinase (PI3K), and the GEFs for the small G-protein Ral pathway (RalGEF). The raf kinases are involved in the prominent Ras-Raf-MEK-ERK pathway. This pathway consists of several phosphorylation events including the three kinases, namely Raf, MEK (MAP kinase kinase), and ERK (MAP kinase) [18]. After phosphorylation of ERK, it immediately translocates into the nucleus and activates transcription factors (e.g. ELK1) that directly or indirectly promote the expression of cyclin D, a protein involved in cell cycle progression [19-20]. A second pathway initiated by Ras-GTP is triggered by the activation of PI3K [21]. Activated PI3K is attached to the plasma membrane and phosphorylates phosphatidylinositol-4,5-bisphosphate (PIP2) to generate phosphatidylinositol-3,4,5-triphosphate (PIP3). The second messenger PIP3 then activates 3-phosphoinositide-dependent protein kinase 1 (PDK1) and Akt [22]. Activated Akt kinase promotes survival by inactivating pro-apoptotic proteins like BAD and the forkhead transcription factor (FKHR) [23]. Since all these kinases involved in downstream Ras signaling are important to transfer signals from the periphery to the nucleus, they are regarded as potential targets in anti-cancer therapy to inhibit tumor cell proliferation or survival promoted by oncogenic Ras [18, 24]. This is an interesting fact, because in about 30% of all human cancers constitutively active Ras molecules (K-Ras > N-Ras > H-Ras) can be found, causing permanent signaling and sustained cell proliferation (Tab. 1) [25].
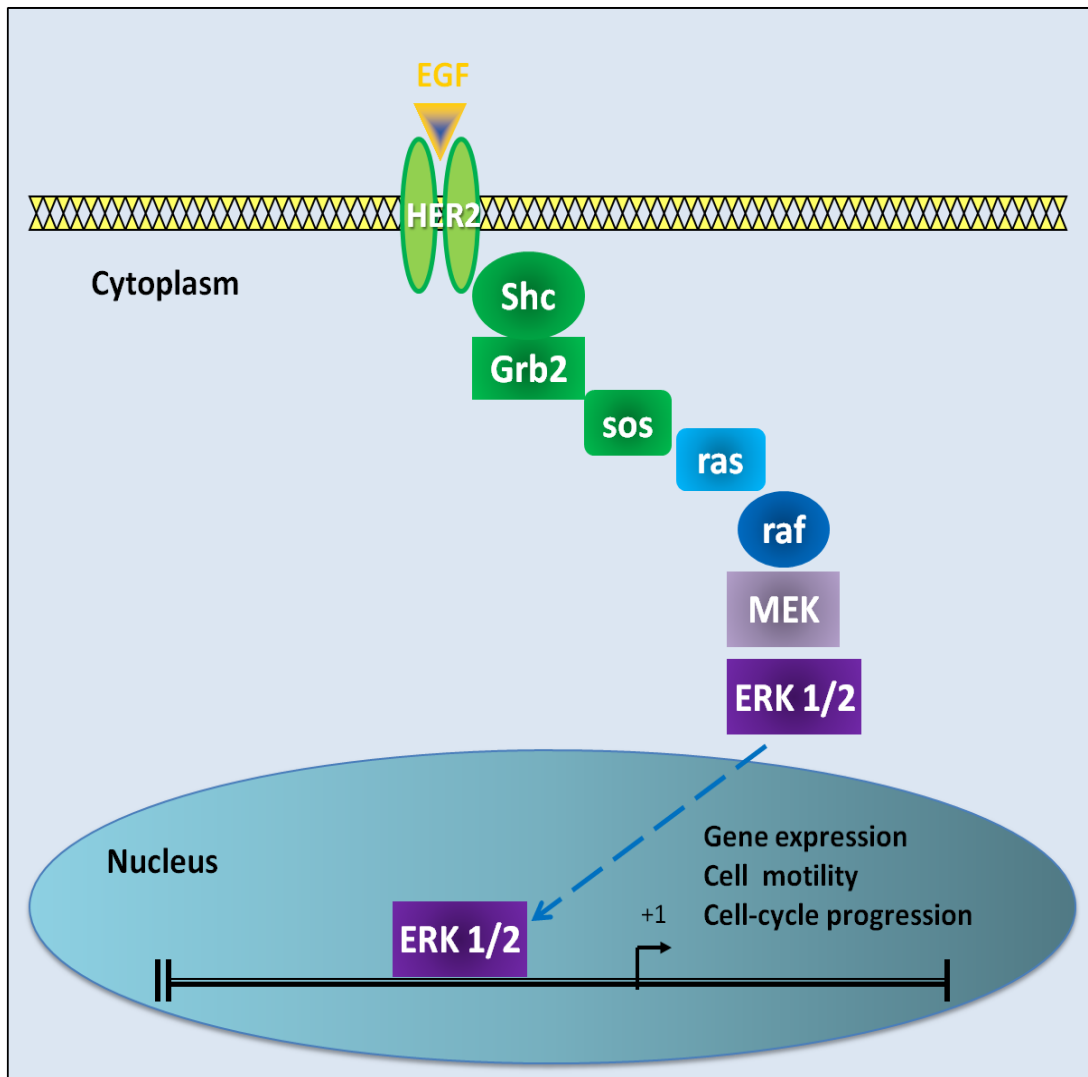
Fig. 3: The EGF signaling pathway involving Ras activation:

Binding of EGF to its receptor HER2 leads to dimerization and autophosphorylation of the receptor followed by recruitment of Shc and Grb2. Subsequently, the GEF molecule SOS is bound and activates Ras by exchanging GDP with GTP. Activated Ras triggers the prominent Ras-Raf-MEK-ERK cascade which results in cell responses such as gene expression, cell motility and cell-cycle progression. Figure adapted from [26].

Although Ras molecules have an intrinsic GTPase activity that leads to hydrolyzation of bound GTP to GDP there are GTPase activating proteins (GAPs) that accelerate the process of inactivation. This is of importance as the Ras-GDP/GTP levels have to be controlled precisely [27] (Fig. 4).
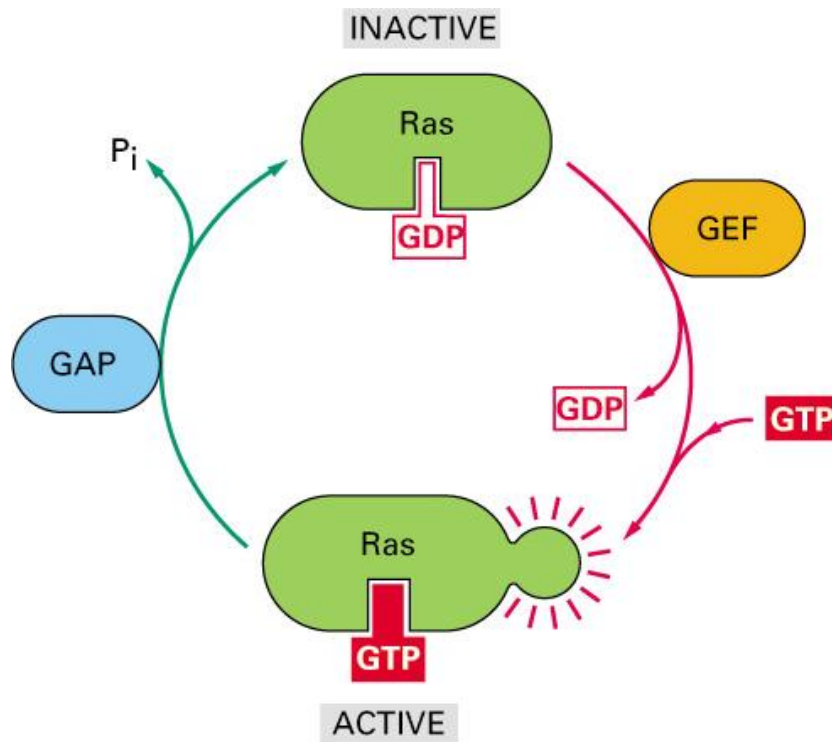
Fig. 4: Activation / Inactivation cycle of Ras proteins:

GEF molecules (e.g. SOS) bind to inactive GDP-bound Ras and trigger the release of the GDP nucleotide by inducing conformational changes in the P loop and switch regions. Ras can now bind the more abundant GTP nucleotide and this leads to the displacement of the GEF molecule at the same time. Although Ras has an intrinsic GTPase activity GAP molecules are necessary to precisely regulate the signaling capacity by binding to activated Ras and initiating the hydrolyzation of GTP to GDP in order to terminate the signal. Figure adapted from [28].

1.1.3 Ras and its role in cancer – mechanism and treatment approaches

Being a proto-oncogene hyper-active Ras (oncogenic Ras) plays a crucial role in several types of cancer and in developmental defects such as Noonan, Costello and cardio-facio-cutaneous (CFC) syndromes [25]. K-Ras is frequently mutated in pancreatic, colorectal, endometrial, biliary tract, lung and ovarian cancers. Both K-Ras and N-Ras mutations are found in myeloid malignancies. Melanoma and bladder cancer are known for having N-Ras and H-Ras mutations [29-30] (Tab. 1). These defects are characterized by the following frequent mutations that lead to a constitutively active Ras unable to perform hydrolysis to transform the bound GTP into GDP: This occurs when the glycine (G) on position 12 or 13 in the P-loop is mutated into valine (V). After this mutation GAP recognition is not possible and Ras inactivation cannot take place [31]. A further prominent mutation is related to the glutamine (Q) on position 61 in the catalytic center. If this amino acid is changed into a lysine (K) or arginine (R) residue the transition state for GTP hydrolysis cannot be stabilized and

13

elimination of the γ-phosphate cannot be achieved [32]. These defects keep the protein in a permanent 'on' state and lead to sustained signaling.

Several approaches have been investigated to target oncogenic Ras in cancer. As described above (in 1.1.1) post-translational modifications are necessary to locate the Ras protein at the plasma membrane. This is the reason why farnesyltransferase inhibitors (FTIs) were elaborated and tested as cancer therapeutics. However, when farnesylation is blocked the tumor cell may switch to geranylgeranylation as post-translational modification. This can only be observed for K-Ras and N-Ras; H-Ras is exlusively modified by farnesyltransferase. The fact of having 20 carbon atoms instead of 15 as membrane anchor did not alter the biological activity of Ras [30]. Using both inhibitors, one for farnesylation and one for geranylgeranylation, did not yield superior results because of very high toxicity [33]. Further studies have been performed to develop antisense oligonucleotides against Ras or Raf. These drugs were tested in clinical trials, but failed due to several problems like specificity, delivery to only malignant cells and sufficient uptake [34]. The development of drugs inhibiting upstream or downstream targets of Ras is also under investigation. In this context PD98059 (MEK inhibitor) and U0126 (MEK inhibitor) were widely used in clinical research and CI-1040 (former PD184352; MEK inhibitor) has also undergone clinical trials [35-37]. Targeting upstream components of the Ras signaling cascade includes small-molecule tyrosine kinase inhibitors and humanized antibodies against the receptor extracellular domains (e.g. cetuximab, herceptin) [38-40]. Of note, these approaches are limited to cancer patients with aberrant receptor activation but wild type Ras configuration.

Cancer type	HRAS	KRAS	NRAS
Biliary tract	0%	33%	1%
Bladder	11%	4%	3%
Breast	0%	4%	0%
Cervix	9%	9%	1%
Colon	0%	32%	3%
Endometrial	1%	15%	0%
Kidney	0%	1%	0%
Liver	0%	8%	10%
Lung	1%	19%	1%
Melanoma	6%	2%	18%
Myeloid leukaemia	0%	5%	14%
Ovarian	0%	17%	4%
Pancreas	0%	60%	2%
Thyroid	5%	4%	7%

Tab. 1: H-Ras, K-Ras and N-Ras mutations in human cancer:

Data were taken from the Sanger Institute Catalogue of Somatic Mutations in Cancer [25, 41].

1.2 Intercellular protein transfer

Classical theories of cell autonomy and the assumption that each cell is an island are questioned by the discovery of new types of cell-cell communication pathways. These new pathways involve "proteome mixing" especially in the case of immune cells, and represent novel possibilities of cell-cell interaction which challenge the idea of cell identity and autonomy [42]. In the next introductory part three different mechanisms of intercellular protein exchange (based on exosomes, nanotubes, and trogocytosis) will be described and a special focus will be placed on trogocytosis.

1.2.1 Mechanisms of intercellular protein transfer

1.2.1.1 Exosomes

Eukaryotic cells can release phospholipid-enclosed vesicles into their environment. These vesicles do not simply constitute cellular debris but these so called exosomes are membrane vesicles actively released by cells upon fusion of multivesicular bodies / endosomes (MVBs / MVEs) with the plasma membrane or directly shed off the plasma membrane [43-45]. Exosomes harbor a unique set of proteins such as endosomal–lysosomal sorting proteins (Alix, Tsg101), tetraspanins (CD63, CD9, CD81) and heat-shock proteins (Hsp70 and Hsp90) but also nucleic acids [44-47]. Upon interaction with the target cell, exosomes fuse with the cell membrane and thereby transfer their components onto the recipient cell (Fig. 5). This way of molecule exchange enables a cell contact independent way of cell to cell communication [48]. The secretion of these vesicles is not intended to get rid of obsolete particles, but several findings, especially regarding the immune system, suggest that exosomes contribute to the cross-talk between different cells and cell types [49-50]. Shedding of microparticles such as exosomes is also observed by tumor cells and may result in the alteration ("education") of the tumor microenvironment and immune response. Furthermore, exosome shedding by tumors has been addressed in developing new therapeutics or biomarkers for rapid diagnosis [51-52].
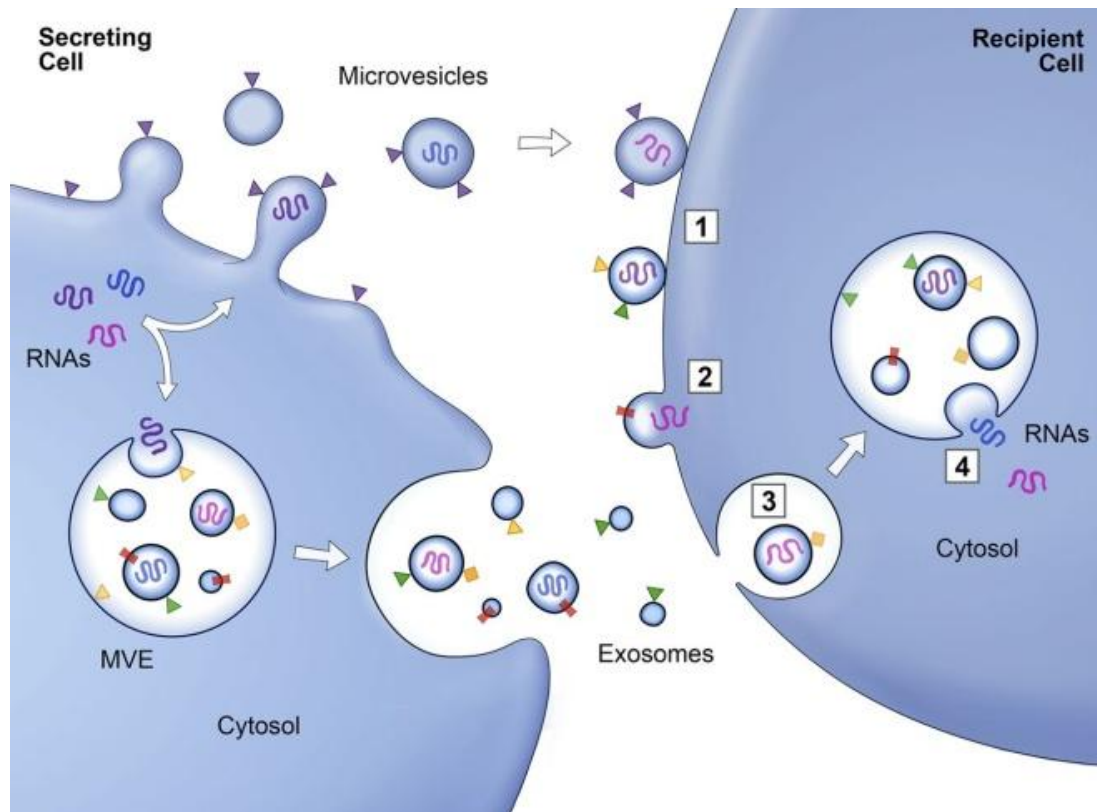
Fig. 5: Formation, shedding and uptake of exosomes:

Secreting cells (left) form MVBs or MVEs (multivesicular bodies / endosomes) containing different molecules such as membrane-associated or transmembrane proteins and RNAs. These vesicles bud from the plasma membrane and can be taken up by recipient cells (right) via different ways: (1 and 2) Direct fusion with the plasma membrane of the acceptor cell. (3 and 4) Intracellular fusion of endocytosed exosomes with the membrane of endocytic compartments. All described pathways result in cargo (protein or RNA) release into the recipient cell. Figure adapted from [53].

1.2.1.2 Nanotubes

Discovered by in vitro studies tunneling nanotubes (TNTs) were described as having a diameter of 50–200 nm and a length up to several cell diameters [54]. Chinnery et al. could show that TNTs are also present in vivo and lead to intercellular communication, environmental sampling, and protein transfer [55]. Functions range from signaling via calcium fluxes to the transfer of cytoplasmic vesicles and cell surface proteins including MHC (major histocompatibility cluster) class I molecules or B-cell receptor/antigen complexes [56-57]. Also pathological functions have been observed: TNTs are employed by retroviruses that can induce the formation of filopodia and use nanotubes as a novel route to infect connected cells [58-59]. Other pathogens such as bacteria are also linked to TNTs and may move along the outside of nanotubes [60]. It is further reported that different cell types have distinct types of TNTs and that the molecule composition and function of these tubes can vary (Fig. 6) [60-61]. The de novo TNT formation only takes a few minutes and is

16

conducted via two different mechanisms: on the one side actin polymerization drives the outgrowth of a filopodia-like protrusion to a neighboring cell and on the other side TNTs are formed when attached cells separate again [56, 59, 62].
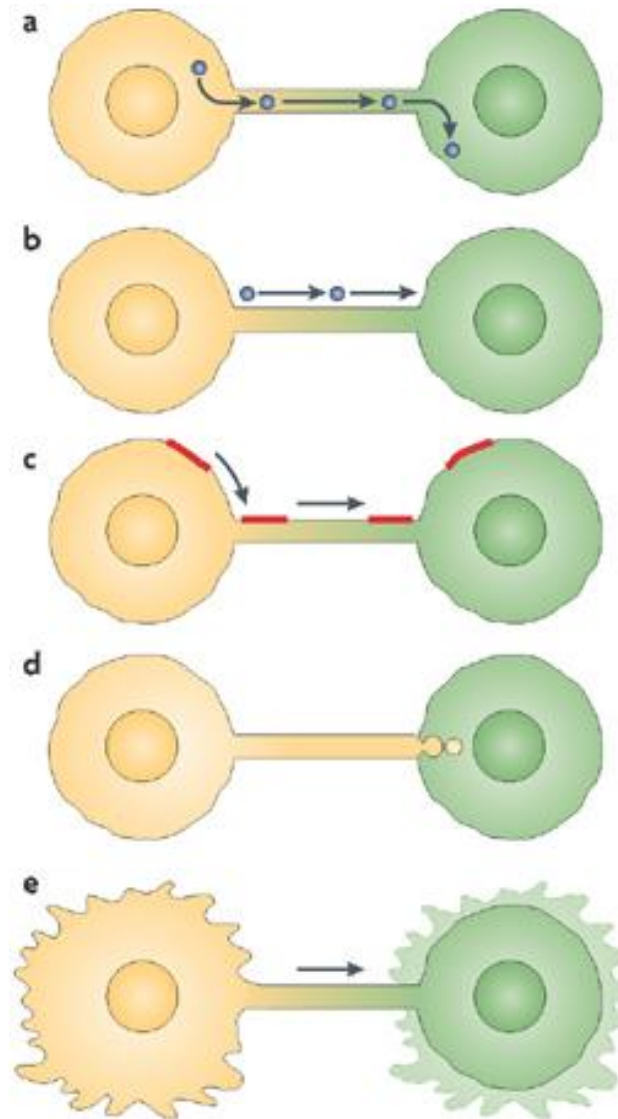
Fig. 6: Molecule exchange between cells via intercellular tunneling nanotubes:

(a) Cargo particles such as vesicles or large molecules can be transported within open-ended nanotubes. (b) Cargo molecules are also transported on the outside of the tunneling nanotube which has been described for bacteria or viral particles. (c) Whole membrane patches with transmembrane proteins are transferred via tunneling nanotubes. (d) Endocytic forces tear off parts of the tunneling nanotube and this leads to the exchange of cargo molecules. (e) Small molecules such as ions are transmitted between cells within tunneling nanotubes. Figure adapted from [61].

1.2.1.3 Trogocytosis

Trogocytosis (Fig. 7), coming from the ancient Greek term *trogo* meaning "to gnaw", was first observed in the immunological synapse (IS) between T- and B-cells [63]. During this close cell-cell contact lymphocytes can acquire whole membrane patches containing surface molecules (e.g. the T-cell receptor TCR, MHC I or MHC II) and also plasma membrane located molecules (e.g. Ras) from the antigen-presenting cell (APC) [64-65]. By this way it is possible for a recipient cell to obtain molecules that are not expressed by the cell itself and can directly or indirectly influence the phenotype and function of the acceptor cell. This phenomenon does not only occur in vitro but also in vivo and has been documented for T-, B- and natural killer (NK) cells [66-68]. Scientists have proposed that this new mechanism of cell to cell communication shapes the induction and regulation of immune responses. Due to its rapid speed (within minutes) of protein transfer between a donor and an acceptor cell, phagocytosis or apoptotic bodies as the mechanism of action have been excluded [64, 69]. Negative consequences of this exchange of whole membrane patches and its associated molecules could be the distribution of pathogens or their surface receptors (e.g. prions or receptors for human immunodeficiency virus) [68].

Another aspect of trogocytosis reported by Hudrisier et al. is that cells that perform trogocytosis have to be equipped with specific surface receptors. T-cell molecules for instance that trigger trogocytosis are TCR, CD3 and CD28 [66]. However, it remains unclear why certain receptors trigger trogocytosis while others do not. Aucher et al. found that T-cells also require signaling by Src-kinase, Syk-kinase, and PI3K for efficient trogocytosis [70]. Moreover, it was reported that both, the acceptor cell and the donor cell have to have an active cytoskeleton. This fact could be demonstrated by using the drug latrunculin B which inhibits actin polymerization. Pre-incubation of the interacting cells with latrunculin B resulted in a lower transfer of membrane molecules by trogocytosis, in particular for T-cells [67, 71].
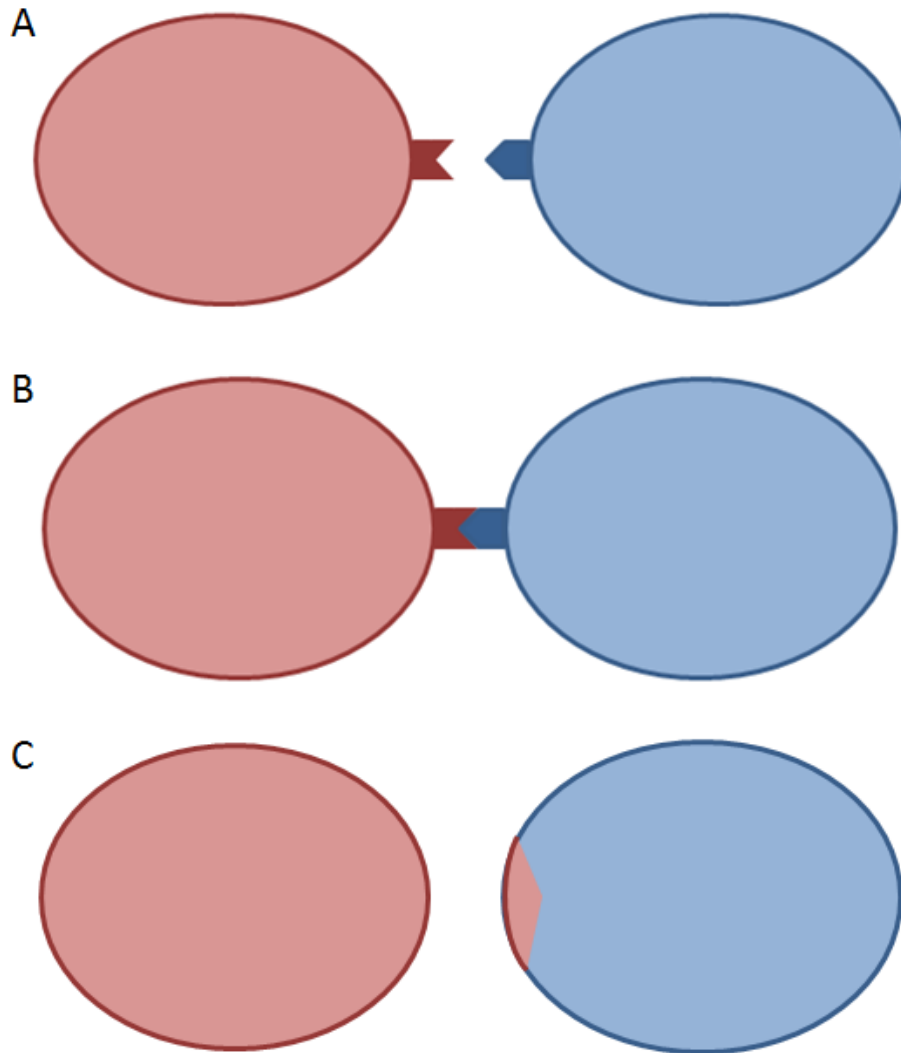
Fig. 7: Schematic illustration of trogocytosis:

(A) Donor and acceptor cell are illustrated in red and blue, respectively. (B) Donor cell and acceptor cell get in close contact. (C) A whole membrane patch is transferred from the donor cell to the acceptor cell.

1.2.2 Transfer of membrane-associated signaling molecules such as Ras

In 2007 Rechavi et al. were the first to report the exchange of membrane-associated signaling molecules between lymphocytes [65]. After co-culture of NK-cells or CD3^{+} T-cells with stably transfected B-cells expressing a fusion of enhanced green fluorescent protein (EGFP) and oncogenic H-Ras (EGFP-HRasG12V) 40-60% of the recipient NK- and T-cells were found EGFP positive which indicated Ras protein transfer.

The transfer occurred very rapidly (i.e. was detectable within 15 min) and resulted in a considerable amount of EGFP-HRas exchange as illustrated by a high mean fluorescence intensity (MFI) of acceptor cells [65]. Compared to the intercellular protein exchange via exosomes or TNTs, the transfer of EGFP-Ras proteins was substantially faster which indicated a transfer mechanism by trogocytosis. This notion was further supported by inhibition of EGFP-Ras transfer in the presence of latrunculin B.

Furthermore, it was of interest that EGFP fusion to the C-terminal membrane anchor of Ras was sufficient to mediate protein transfer, i.e., protein exchange was not dependent on a functional Ras molecule but was promoted by the membrane association of the molecule.

Using surface and intracellular staining, flow cytometry as well as confocal laser scanning microscopy (CLSM) the authors could show that transferred EGFP-HRasG12V was located on the inner side of the plasma membrane. This data conforms with results presented by McCann et al. who reported that transferred membrane proteins retained their orientation and functional properties [72]. Comparably, Rechavi et al. documented functional consequences of Ras protein transfer, as pERK activation could be shown in the recipient NK-cells after co-culture with EGFP-HRasG12V expressing B-cells [65]. It is well documented by scientific literature that activated pERK leads to enhanced cytokine secretion and cell proliferation of lymphocytes [70, 72]. These functional consequences could also be observed following EGFP-HRas transfer into NK- or T-cells.

When investigating other acceptor cells than lymphocytes, Rechavi et al. found that the uptake of EGFP-HRasG12V was mainly a lymphocytic characteristic while other non-lymphoid cell types could function as donor cells [65]. A later study also demonstrated that oncogenic Ras was transferred from tumor cells to recipient lymphocytes [73]. However, these analyses did not include Ras protein transfer from or to endothelial cells which has been chosen as the focus of the present master thesis.

1.3 Preliminary work

The master project was based on the hypothesis that endothelial cells (ECs) may function as recipient cells for Ras protein transfer. Since they constitute a barrier between blood, lymph and tissue which is traversed by immune cells during diapedesis or by tumor cells during metastasis, ECs come in close contact with the transmigrating cell populations. This may indeed favor the exchange of membrane proteins such as Ras. Of particular interest, the transfer of oncogenic Ras from tumor cells onto endothelial cells could possibly alter the EC phenotype and function in a metastatic setting.

In different experiments three main questions were to be addressed. The first question was if Ras proteins were transferred from tumor cells onto the recipient endothelial cells. As a next step the membrane localization and orientation of the transferred Ras protein was to be monitored and finally, the potential mechanism of Ras transfer by trogocytosis was to be investigated.

Katrin Gitschtaler, MSc performed the initial work for this study and achieved the following results [74]: The T-cell lymphoma Jurkat line which does not harbor any endogenous Ras gene mutations [75] was stably transfected with different EGFP-Ras fusion constructs which were generously supplied by our collaboration partners Yoel Kloog and Oded Rechavi (Fig. 8). Besides the characterization of the stably transfected Jurkat clones a trans-endothelial migration (TEM) assay was established. This was followed by flow cytometric analysis of endothelial cells after tumor cell transmigration and showed that the EGFP-Ras protein was transferred from Jurkat cells onto ECs. Transfer efficiency was, however, very low and generally observed in less than 5% of endothelial cells. Katrin Gitschtaler further demonstrated that the transferred EGFP-Ras molecule was located at the inner side of the plasma membrane i.e. retained its proper membrane orientation. Optimization of the TEM assay was carried out in terms of cell ratio (ECs to Jurkat cells), time of co-culture, transwell (TW) size and pre-stimulation of the cells. Experiments were also performed with transiently transfected Jurkat cells. Although a higher EGFP-Ras transfer to ECs could be observed with transiently transfected Jurkat cells, stably transfected clones were used for further experiments, because of a more physiological setup (i.e. lower Ras expression levels as would be expected in vivo). Katrin Gitschtaler further established that cell-cell contact was required for Ras transfer from Jurkat cells to ECs. To check for trogocytosis a lipophilic dye (DiR) was introduced in co-culture experiments. Surprisingly, the Jurkat to EC transfer of the membrane

dye and the transfer of the EGFP-Ras protein did not correlate well. This led to the assumption that trogocytosis may not necessarily be the mechanisms of action in Ras transfer from Jurkat to endothelial cells.

Comparable experiments were performed by Katrin Gitschtaler with SK-BR-3 epithelial breast cancer cells which were derived from a solid tumor and therefore likely to exhibit properties distinct from lymphoma cells. For these experiments SK-BR-3 cells were stably transfected with EGFP-Ras constructs as had been done for the Jurkat cells. After optimization of the TEM assay the result of the Ras transfer from breast cancer cells into ECs was essentially negative. Because of the previous report on Ras transfer from melanoma cells to T lymphocytes [67, 73], a co-culture of SK-BR-3 cells and PBMCs (peripheral blood mononuclear cells) was performed. This led to a massive EGFP-Ras transfer from breast cancer cells to lymphocytes and monocytes. Katrin Gitschtaler therefore concluded that EGFP-Ras transfer required a leukocyte component. While oncogenic Ras could be transferred from lymphoma Jurkat cells onto ECs, the oncogenic Ras of epithelial breast cancer cells could only be passed on to leukocytes but not to endothelial cells. Thus, all subsequent experiments of the present master study were focused on the Jurkat-EC model.
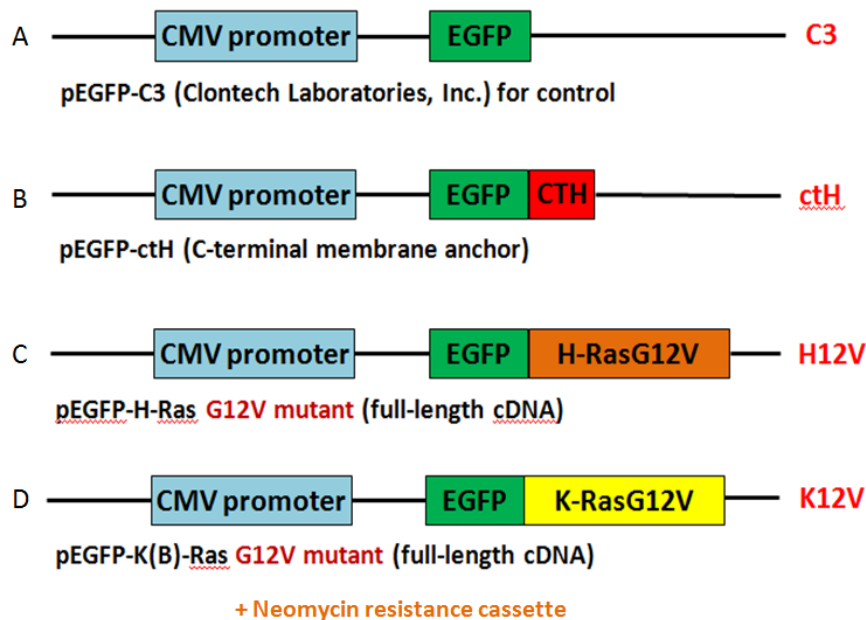
Fig. 8: EGFP-Ras expression constructs applied to test intercellular Ras protein transfer:

All four expression constructs contain a cytomegalovirus promoter (CMV) and a neomycin resistance cassette. The promoter is followed by the coding sequence for EGFP fused in frame to the 5´ end of Ras isoforms. (A) The C3 construct that only encodes EGFP serves as a negative control. (B) The ctH construct contains an EGFP sequence fused to the membrane anchor region of H-Ras which enables the fusion protein to insert into the plasma membrane but cannot trigger Ras signaling. (C and D) The last two constructs cover the EGFP fusion with full-length, oncogenic H-Ras or K(B)-Ras with a glycine to valine mutation in position 12 that leads to a constitutively active Ras protein.

1.4 Aims of the study

Preliminary work showed that there is a transfer of EGFP-Ras molecules from stably transfected tumor cells (Jurkat clones) to endothelial cells during a transmigration experiment mimicking the process of tumor cell extravasation. This master study was designed to gain deeper insight into this process. Several experiments previously conducted by Katrin Gitschtaler were repeated and additional, novel questions were addressed as follows:

1.) Can intercellular exchange of Ras molecules between Jurkat cells and endothelial cells be verified?

a) Is the Ras exchange observed at physiological cell ratios or does it only occur when tumor cells are present in excess?

b) What is the cellular localization of transferred Ras?

c) What is the time course of Ras exchange?

d) What is the half-life of the transferred Ras molecules?

2. What is the mechanism of Ras transfer from Jurkat cells to ECs?

a) Is trogocytosis the mode of action: can the exchange of whole membrane patches be demonstrated by transfer of the lipophilic dye PKH67?

b) Can Ras transfer be reduced or blocked by the filament disrupter latrunculin B?

3. Does Ras transfer from tumor cells to ECs result in any functional consequences?

a) Is there enhanced signaling (pERK) in ECs upon uptake of oncogenic Ras molecules?

2. MATERIALS AND METHODS

2.1 Ethics statement

This laboratory investigation involved primary cells retrieved from human tissue and was conducted according to the principles expressed in the Declaration of Helsinki. The isolation of cells was approved by the institutional "Ethics Committee of the Medical University of Vienna" (#1123/2009); all volunteers or legal representatives gave written informed consent.

2.2 Cell culture

Incubators containing a humidified atmosphere with 5% CO_2 at 37°C were used for cell culturing. For in vitro experiments involving eukaryotic cells sterile conditions and sterile equipment were utilized.

2.2.1 Primary human cells, cell lines and clones

Human microvascular endothelial cells (HMECs):
- Lymphatic endothelial cells (LECs)

Human carcinoma cell lines and clones:
- Jurkat cells (clone E6-1, ATCC® TIB-152™)
- Jurkat C3 clone_1G11
- Jurkat ctH clone_4G11
- Jurkat H12V clone_1G4
- Jurkat K12V clone_1B7

All stably transfected Jurkat clones were generated by Katrin Gitschtaler, MSc as previously described [74].

2.2.2 Cultivation of Jurkat cells and stably transfected clones

Jurkat cells were cultured in RPMI-1640 growth medium and split 1:5 or 1:10 every two to three days by diluting the cell suspension in growth medium. Stably transfected clones were treated similarly but 2 mg/ml G418 were added to the culture medium. Cells were changed to RPMI-1640 growth medium without G418 two to three days prior to each experiment.

2.2.3 Isolation and cultivation of human microvascular endothelial cells

Isolation and purification of endothelial cells was kindly performed by our technician Anna Zommer. Human foreskin samples retrieved from the General Hospital of Vienna were digested with dispase and resulting cell isolates were put in culture. In brief, endothelial cells and fibroblasts were purified with antibody-coupled magnetic beads. To separate lymphatic endothelial cells podoplanin was used as the appropriate surface marker. Blood endothelial cells (BECs) and non-EC types (mainly fibroblasts) that remained in the cell fraction were further separated by using an antibody against CD31 which is located on the surface of BEC cells. After further cell culture the isolated endothelial cells were characterized by flow cytometry for the expression of podoplanin and CD31 using fluorescence-labeled antibodies. Activation of HMECs was also determined by analysis of CD62E and CD54 expression after EC stimulation with tumor necrosis factor alpha for 4 h. Only isolates with a purity greater than 98% were used for subsequent experiments.

For cell culturing flasks of different sizes (T25, T75 and T150 cm^2) were used with the appropriate amount of reagents as listed in Tab. 2. Endothelial cells were split two or three times a week at a ratio of 1:2 or 1:3 depending on the state of confluence. The current medium was removed, cells were washed with an appropriate amount of PBSdef (phosphate-buffered saline without Ca^{2+} and Mg^{2+}) and detached by adding 1x trypsin-EDTA (ethylene diamine tetraacetic acid). An incubation step of about 5 min at 37°C followed and the same amount of 10% FCS (fetal calf serum) in PBSdef was added to stop the proteolytic digest. The cell suspension containing the detached cells was transferred into a 50 ml reaction tube. To increase the number of harvested cells the empty flask was rinsed with 10% FCS in PBSdef one or two times. Centrifugation (330 x g, 5 min) at room temperature (RT) followed. The cell pellet was resuspended in endothelial growth medium without vascular endothelial

growth factor (EGM-2-MV w/o VEGF), split and transferred into a new cell culture flask. New flasks were pretreated for 5 min at RT with 0.2% gelatin in PBSdef.

Flask (cm²)	0.2% gelatin (ml)	1x trypsin-EDTA (ml)	10% FCS in PBSdef (ml)	medium (ml)
6-well	1	1	1	2
T25	1	1	1	4
T75	3	3	3	10
T150	6	6	6	20

Tab. 2: List of reagent volumes applied in standard cell culture

Materials

Cell culture media and solutions:

EGM-2-MV w/o VEGF*:*

    EBM-2 basal medium (500 ml)

    + 5% heat inactivated FCS

    + hydrocortisone

    + ascorbic acid

    + gentamicin/amphotericin

    + R3-hIGF-1

    + hFGF-B

    + hEGF

Clonetics,

Cambrex Bio Science Walkersville, Inc.

Walkersville, MD, USA

(concentrations not specified)

RPMI-1640 growth medium*:*

    RPMI-1640 with GlutaMAX™

    + 10% heat inactivated FCS

    + 1 mM sodium pyruvate   (stock: 100 mM)

    + 2.5 mg/ml D-glucose   (stock: 250 mg/ml)

    + 100 µg/ml streptomycin   (stock: 10000 µg/ml)

    + 100 U/ml penicillin   (stock: 10000 U/ml)

Invitrogen,

Carlsbad, CA, USA

RPMI-1640 growth medium with G418:

     RPMI-1640 with GlutaMAX™

     + 10% heat inactivated FCS

     + 1 mM sodium pyruvate   (stock: 100 mM)

     + 2.5mg/ml D-glucose   (stock: 250 mg/ml)

     + 100 µg/ml streptomycin   (stock: 10000 µg/ml)   Invitrogen,

     + 100 U/ml penicillin   (stock: 10000 U/ml)   Carlsbad, CA, USA

     + 25 mM HEPES   (stock: 1 M)

     + 2 mg/ml G418 (neomycin analogue)

1 g of G418 (neomycin analogue) was added to 500 ml RPMI-1640 with GlutaMAX™. After G418 was dissolved, the medium was sterile-filtered (0.2 µm) and all other components were added thereafter.

10x trypsin-EDTA (0.5% trypsin, 5.3 mM EDTA*Na)

1x trypsin-EDTA (working solution):   Invitrogen,

     10x trypsin-EDTA diluted in PBSdef (1:10)   Carlsbad, CA, USA

PBSdef (Ca^{2+} / Mg^{2+}-free)   (PAA, Pasching, Austria)

Fetal calf serum   (Linaris, Wertheim – Bettingen, Germany)

Formaldehyde   (Sigma-Aldrich, St. Louis, MO, USA)

Gelatin solution type B (2% in H_2O)   (Sigma-Aldrich, St. Louis, MO, USA)

10% FCS in PBSdef (working solution): 50 ml FCS in 500 ml PBSdef

5% FCS in PBSdef (working solution): 10% FCS in PBSdef diluted with PBSdef (1:2)

0.2% gelatin in PBSdef: 50 ml 2% gelatin solution type B in 500 ml PBSdef

Reagents for endothelial cell isolation and purification:

CELLection[TM] Pan Mouse IgG Kit including 50 – 60 U/µl DNase

     (Dynal Biotech, Oslo, Norway)

100 U/ml collagenase CLS-2 solution in PBSdef   (Worthington Biochemical

     Corp., Lakewood, NJ, USA)

Dispase 50 U/ml   (Collaborative Biomedical Products, Bedford, USA)

Antibodies for cell purification and quality control:

anti-hCD31, mIgG1, clone WM59, MCA1738   (Serotec, Oxford, UK)

anti-podoplanin, mIgG1, clone 18H5, ab10288   (Abcam, Cambridge, UK)

mIgG1-FITC, isotype control   (Serotec MCA928F (1:100)

anti-hCD54-FITC, mIgG1   (Serotec MCA532F (1:100)

anti-hCD62E/P-FITC, mIgG1   (Serotec MCA883F (1:100)

mIgG1-PE, isotype control   (Serotec MCA928PE (1:20)

anti-hCD31-PE, mIgG1   (Serotec MCA1738PE (1:20)

anti-hCD34-PE, mIgG1   (Serotec MCA1578PE (1:20)

Plastic equipment:

TPP® 6-well tissue culture (TC)-treated microplates (30 mm wells)

TPP® 12-well TC-treated microplates

TPP® 24-well TC-treated microplates   TPP,

TPP® 96-well clear, round bottom microplates   Trasadingen,

TPP® triangular angled neck cell culture flask with vent cap (T25, T75, T150)   Switzerland

Reaction tube 50 ml and 15 ml w/o skirt   (Sarstedt AG, Nümbrecht, Germany)

CORNING® 100 mm TC-treated culture dish   (Corning Inc., Corning, NY, USA)

Reaction tube 1.5 ml   (Greiner Bio-One, Frickenhausen, Germany)

Reaction tube 2 ml   (Eppendorf, Hamburg, Germany)

Cellstar®, polypropylene FACS tubes   (Greiner Bio-One, Frickenhausen, Germany)

2.3 Trans-endothelial migration assay with Jurkat cells or clones

2.3.1 Day 1 - Preparation of endothelial cells

On the first day of the experiment ECs were seeded onto the upper side of transwells (TWs). ECs were harvested from culture flasks via detachment with 1x trypsin-EDTA, counted and

set to a concentration of 6.25×10^5/ml in EGM2-MV w/o VEGF + fibronectin (4 µl/ml). Transwells (8 µm pore size) were placed into 6-well plates, 800 µl cell suspension (5×10^5 ECs) were carefully added and equally distributed to ensure complete coverage of the transwell after 24 h. The cells were left at 37°C to let the cells settle onto the TW. After 4 h of incubation the medium was removed, cells were washed with 1 ml PBSdef and 800 µl of EGM2-MV w/o GFs (growth factors) were added to the upper compartment and 2.5 ml of EGM2-MV w/o GFs were added to the lower compartment. The 6-well plate containing the transwells was incubated over night at 37°C.

2.3.2 Day 2 - Preparation and addition of tumor cells

Activation of Jurkat cells or clones with cytokines:
Jurkat cells or clones cultured in growth medium without G418 were mixed thoroughly and counted. Cells were set to a concentration of 2×10^6 cells/ml in EGM2-MV w/o GFs. 1.25 ml (2.5×10^6 cells) were transferred into a 1.5 ml Eppendorf tube. Interleukin-1β (IL1β, 100 pg/ml) and interferon-γ (IFNγ, 2.5 U/ml) were added and the cells were incubated for 4 h at 37°C under gentle rotation.

Jurkat Trans-Endothelial Migration:
After 4 h of activation Jurkat cells or clones were centrifuged and resuspended in 800 µl EBM-2 + 0.1% BSA. The EC medium was removed from transwells, ECs were washed apically with 1 ml PBSdef and the resuspended Jurkat cells were added. The subsequent incubation period ranged from 15 min to 4 h.

2.3.3 Harvesting procedure

ECs and the adherent Jurkat cells were harvested from transwells. Thus, apical and basal medium was removed and the TWs were washed with 1 ml PBSdef. 600 µl of accutase (diluted 1:2 with PBSdef) were added to the upper compartment and an incubation step of 5 min at 37°C followed. To stop the reaction 600 µl of 10% FCS in PBSdef were added. Cells were removed from the TW and transferred into micron tubes. If the cells did not detach easily, a cell scraper was used to carefully scratch off the cells from TWs.

2.3.4 Detection of transferred EGFP-Ras by flow cytometry

Micron tubes were centrifuged at 480 x g for 3 min at room temperature (RT) and the supernatant was removed. The cell pellet was resuspended in 1 ml PBSdef containing 1 µl of brilliant violet dye (LIVE/DEAD Fixable Violet Dead Cell Stain Kit) to allow for distinction between living and dead cells in flow cytometric analysis. After 30 min of incubation at RT in the dark the micron tubes were centrifuged again and the pellet was washed with 1 ml PBSdef.

The first antibody solution for immunolabeling of ECs and Jurkat cells contained mouse anti-human CD146-biotin (1:1000) in 5% FCS in PBSdef. The pellet was resuspended in 100 µl and incubated at 4°C for 20 min. Afterwards 1 ml 5% FCS in PBSdef was added and the micron tubes were centrifuged at 480 x g for 3 min at RT. The second antibody solution contained a conjugate of streptavidin with PE-TexasRed (1:500) and mouse anti-CD45-PC5 (1:20) in 5% FCS in PBSdef. Again, the cell pellet was resuspended in 100 µl and incubation took place at 4°C for 20 min. After washing the cells with 1 ml 5% FCS in PBSdef, 100 µl of Fixation Buffer (Buffer 1; Intraprep Permeabilization Kit) were added and the micron tubes were vortexed thoroughly. After 15 min of incubation in the dark at RT, 1 ml PBSdef was added and the micron tubes were centrifuged as before. For intracellular staining the antibodies were diluted in a 1:1 solution of PBSdef and Permeabilization Buffer (Buffer 2; Intraprep Permeabilization Kit): The cell pellets were carefully covered with 100 µl of rabbit anti-EGFP (1:100). After 5 min the micron tubes were tapped by finger to loosen the pellet and were incubated for another 15 min. A washing step with 1 ml PBSdef and centrifugation followed, and the same procedure was repeated with 100 µl goat anti-rabbit Alexa Fluor® 700 (1:1000). Finally, a last washing step with 1 ml PBSdef was performed and the centrifuged cells were resuspended in 200 µl 5% FCS and 200 µl 2x FIX-buffer. Samples were kept at 4°C in the dark until measurement with a Gallios flow cytometer (Beckman Coulter, Brea, CA, USA) was performed.

Materials

Cell culture media and solutions:

EGM2-MV w/o VEGF (see Materials 2.2)

EGM2-MV w/o GFs*:*

EGM-2-MV (see Materials 2.2.3) without supplementation of any growth factors (R3-hIGF-1, hFGF-B, hEGF, hVEGF)

EBM2 + 0.1% BSA:

    EBM-2 basal medium

    + 0.1% BSA   (Sigma-Aldrich, St. Louis, MO, USA)

Accutase 1:2 diluted with PBSdef (working solution)   (PAA, Pasching, Austria)

2x FIX buffer: 6.75 ml of 37% formaldehyde in 500 ml PBSdef

PBSdef

10% FCS in PBSdef
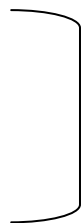
5% FCS in PBSdef   see Materials 2.1.

Human plasma fibronectin (1 mg/ml)   (Chemicon, Temecula, CA, USA)

Fibronectin 0.25 µg/ml (working solution): 1 mg/ml human plasma fibronectin diluted in PBSdef (1:4)

LIVE/DEAD Fixable Violet Dead Cell Stain Kit   (Invitrogen, Carlsbad, CA, USA)

Intraprep Permeabilization Reagent   (Beckman Coulter, Brea, CA, USA)

IL1ß: stock 100 ng/ml → 100 pg/ml f.c. (1:1000)   (R & D Systems, Minneapolis, USA)

IFNγ: stock 500 U/ml → 2.5 U/ml f.c. (1:200)   (Böhringer Ingelheim, Vienna, Austria)

<u>Antibodies:</u>

Mouse anti-human CD146-biotin	(Chemicon, Temecula, CA, USA (1:1000)
Mouse anti-human CD45-PC5 (clone J33)	(Immunotec Inc., Quebec, Canada (1:20)
Rabbit anti-EGFP (IgG)	(Invitrogen, Carlsbad, CA, USA (1:100)
Goat anti-rabbit Alexa Fluor® 700	(Invitrogen, Carlsbad, CA, USA (1:1000)
Streptavidin-PE-TexasRed	(Becton Dickinson, Franklin Lakes, NJ, USA (1:500)

<u>Plastic equipment</u>: see Materials 2.2

Falcon® 8 µm cell culture insert	(Becton Dickinson, Franklin Lakes, NJ, USA)
Falcon® Multiwell™ 6-well plates	(Becton Dickinson, Franklin Lakes, NJ, USA)
Cell scraper	(Sarstedt AG, Nümbrecht, Germany)
Micron tubes	(Micronic, Lelystad, Netherlands)

2.4 Co-culture of endothelial cells and tumor cells

For various analyses (e.g. to investigate the mechanism of EGFP-Ras transfer in detail) the TEM assay was replaced by a simpler co-culture of ECs and tumor cells.

2.4.1 Preparation of ECs and tumor cells

On the first day of the experiment $5x10^5$ ECs were seeded in 2 ml EGM2-MV w/o VEGF medium in a 6-well. After 4 h the medium was changed to EGM2-MV w/o GFs and the cells were incubated at 37°C over night.

Jurkat cells or clones were prepared and activated the following day as described in 2.3.2.

2.4.2 Co-culture and analysis by flow cytometry

On the second day, the ECs in the 6-well were washed with 2 ml PBSdef once. Pre-activated Jurkat cells ($2.5x10^6$ cells) resuspended in 800 µl EBM2 + 0.1% BSA were added to the 6-

well. After 15 min to 4 h of co-culture the cells were harvested and prepared for flow cytometry as described in 2.3.3 and 2.3.4.

<u>**Materials**</u>

<u>Cell culture media and solutions:</u> see Materials 2.2

<u>Plastic equipment:</u> see Materials 2.2

2.5 Intercellular membrane exchange assay based on PKH67

The intercellular exchange of membrane patches was investigated using the lipophilic membrane dye PKH67 in three different approaches: (A) ECs and Jurkat cells separated by a transwell, (B) co-culture of both cell types and (C) incubation of ECs with Jurkat conditioned medium (supernatant).

2.5.1 Preparation of ECs

ECs (5×10^5 per well) were seeded in 6-well plates or TWs (0.1 µm pore size). The medium was changed from EGM2-MV w/o VEGF to EGM2-MV w/o GFs after 4 h of incubation. Then the cells were allowed to form a confluent monolayer over night.

2.5.2 Stimulation of Jurkat cells and PKH67 staining

After pre-stimulation with IL1β and IFNγ (see 2.3.2.) for 4 h at 37°C the Jurkat cells were stained with PKH67. A 4 µM working solution was prepared by diluting 4 µl dye (1 mM stock solution) in 1 ml Diluent C. For staining, 2.5×10^6 Jurkat cells were resuspended in 250 µl Diluent C, 250 µl of the PKH67 working solution were added (final staining concentration: 2 µM PKH67) and mixed immediately by shaking for 1.5 min. 500 µl of FCS were then added and the cells were centrifuged at 330 g for 5 min at RT. Two washing steps with 1 ml 10% FCS in PBSdef and one washing step with PBSdef followed. Finally, the cells were

resuspended in 800 µl EBM2 + 0.1% BSA. Jurkat cells serving as negative control were just resuspended in 800 µl EBM2 + 0.1% BSA and not stained with PKH67.

2.5.3 EC exposure and analysis by flow cytometry

Co-Culture and Transwell Assay (A and B):

To co-culture ECs and Jurkat cells, 2.5×10^6 PKH67-labeled Jurkat cells (in 800 µl EBM2 + 0.1% BSA) were added directly onto the EC monolayer and incubated for 4 h at 37°C. For the transwell assay 7.8×10^6 Jurkat cells (in 2.5 ml EBM2 + 0.1% BSA) were placed into the lower compartment of the TW and also incubated with ECs seeded in the TW for 4 h at 37°C. In both settings, the final Jurkat cell concentration was equivalent to 3.1×10^6 cells/ml.

Tumor Cell Supernatant Assay (C):

To receive the supernatant 2.5×10^6 PKH67-labeled Jurkat cells (in 1 ml EBM2 + 0.1% BSA) were incubated in a 6-well for 4 h at 37°C. The cell suspension was then transferred into a 1.5 ml microtube and centrifuged at 330 g for 5 min at RT. Meanwhile the medium was removed from the ECs (seeded in 6-wells) and the cells were washed with 2 ml PBSdef. Then 800 µl of the Jurkat cell supernatant were added to the EC monolayer for an additional 4 h of incubation.

Immunofluorescence Labeling and Flow Cytometry:

Staining for flow cytometry was performed as described in 2.3.4 with the following modifications: mouse anti-CD146-biotin (1:1000) antibody and secondary reagent streptavidin-PE-TexasRed (1:500) as well as mouse anti-CD45-PC5 (1:20) were used as markers for ECs and Jurkat cells. Live/dead cell stain and antibody against EGFP were not included in this setting i.e. cells were not permeabilized.

2.5.4 Detection of co-transfer of EGFP-Ras and PKH67

When EGFP-Ras transfer was co-investigated with PKH67-labeled membrane exchange, the experimental setting A (co-culture) was recapitulated with EGFP-Ras expressing Jurkat clones. Harvesting and preparation for flow cytometry was performed as described in 2.3.3

and 2.3.4 (i.e. included live/dead cell staining and cell permeabilization for antibody detection of EGFP).

<u>Materials</u>

<u>Cell culture media and solutions:</u> see Materials 2.2

PKH67 Fluorescent Cell Linker (1 mM in ethanol)	(Sigma-Aldrich, St. Louis, MO, USA)
Diluent C	(Sigma-Aldrich, St. Louis, MO, USA)

<u>Plastic equipment:</u> see Materials 2.2

2.6 Detection of surface versus intracellular EGFP-Ras after transfer

2.6.1 Preparation and co-culture of ECs and tumor cells

ECs and Jurkat cells or clones were prepared and exposed to 4 h of co-culture as described above (see 2.4).

2.6.2 Immunostaining and analysis by flow cytometry

The cells were then harvested and stained for flow cytometry as described in 2.3.3 and 2.3.4 with the following modifications: ECs and attached Jurkat cells/clones were harvested from 6-wells, then transferred into micron tubes and centrifuged at 480 x g for 3 min at room temperature. The cell pellet was resuspended in 1 ml PBSdef containing 1 μl of brilliant violet dye. After 30 min of incubation at RT in the dark the micron tubes were centrifuged again and the cells were washed with 1 ml PBSdef. The pellet was resuspended in 500 μl 5% FCS in PBSdef and the suspension was divided into two micron tubes; one for surface and one for intracellular staining.

For surface staining mouse anti-human CD146-biotin (1:1000) and rabbit anti-EGFP (rabbit IgG) (1:100) were diluted in 5% FCS in PBSdef for the first round of antibody incubation of

20 min on 4°C. Cells were washed with 1 ml 5% FCS in PBSdef (and centrifuged at 480 x g for 3 min at RT). For the second round streptavidin conjugated to PE-Texas-Red (1:500), CD45-PC5 (1:20) and Alexa Fluor® 700 goat anti-rabbit IgG (1:1000) were diluted in 5% FCS in PBSdef and incubated for 20 min at 4°C. A last washing step was performed with 1 ml 5% FCS in PBS and finally cells were resuspended in 200 µl of 5% FCS in PBS and 200 µl of 2x FIX buffer.

For intracellular staining the cells were incubated with 100 µl of mouse anti-human CD146-biotin (1:1000) in 5% FCS in PBSdef for 20 min at 4°C. Before the next round of antibody incubation with streptavidin-PE-Texas-Red (1:500) and CD45-PC5 (1:20) followed, the cells were washed with 1 ml 5% FCS in PBSdef. Thereafter, cells were fixed with 100 µl Fixation Buffer (Buffer 1; Intraprep Permeabilization Kit) and incubated for 15 min at RT. After washing with 1 ml PBSdef (and centrifugation at 480 x g for 3 min at RT) the intracellular staining was performed with a 1:1 mix of PBSdef and Permeabilization Buffer (Buffer 2; Intraprep Permeabilization Kit) containing rabbit anti-EGFP (1:100). After 5 min of incubation the micron tubes were carefully tapped by finger and incubated for another 15 min. A washing step with 1 ml PBSdef was followed by the last antibody incubation with Alexa Fluor® 700 goat anti-rabbit IgG (1:1000) in a 1:1 mix of PBSdef and Permeabilization Buffer. Again, after 5 min of incubation the micron tubes were carefully tapped by finger and incubated for another 15 min. Finally, cells were washed with 1 ml PBSdef and suspended in 200 µl of 5% FCS in PBS and 200 µl of 2x FIX buffer and analyzed via flow cytometry.

Materials

Cell culture media and solutions: see Materials 2.2
Plastic equipment: see Materials 2.2

2.7 Intercellular protein transfer in the presence of latrunculin B

2.7.1 Preparation of ECs and tumor cells for co-culture experiments

ECs and Jurkat cells or clones were prepared as described in 2.4. After 3.5 h of Jurkat cell activation with IL1β and IFNγ latrunculin B was added to a final concentration of 1 μM for the remaining 30 min of incubation. ECs were also incubated with 1 μM latrunculin B for 30 min. While Jurkat cells were washed with EBM2 + 0.1% BSA, ECs were washed with PBSdef. Jurkat cells were then resuspended in 800 μl EBM2 + 0.1% BSA and added to the confluent EC monolayer and co-cultured for 30 min. Jurkat and EC suspensions with or without latrunculin B treatment were combined in this set of experiments as outlined in table 3.

LEC -	LEC +	LEC -	LEC +	LEC -	LEC +
Parental -	Parental +	Jurkat clone -	Jurkat clone -	Jurkat clone +	Jurkat clone +

Tab. 3: Experimental setup to test the impact of Jurkat and/or EC treatment with latrunculin B (indicated by +) on intercellular protein transfer using either parental Jurkat cells or an EGFP-Ras expressing Jurkat clone (ctH)

2.7.2 Cell harvesting and analysis by flow cytometry

Harvesting and preparation for flow cytometry was performed as described in 2.3.3 and 2.3.4.

Materials

Cell culture media and solutions: see Materials 2.2

Latrunculin B (2 mM in DMSO)   (Sigma-Aldrich, St. Louis, MO, USA)

DMSO   (Sigma-Aldrich, St. Louis, MO, USA)

Plastic equipment: see Materials 2.2

2.8 Fluorescence-activated cell sorting of EGFP$^+$ ECs

For fluorescence activated cell sorting (FACS) a minimum of $5x10^6$ ECs were co-cultured with stably transfected Jurkat clones. Therefore, ECs were seeded in 10 cm petri dishes ($3.2x10^6$ ECs in 16 ml EGM-2 MV w/o VEGF) and incubated over night at 37°C. Additionally, one 6-well containing $5x10^5$ ECs was prepared for co-culture with parental Jurkat cells. Jurkat cells or clones were again added to EC cultures on the following day at a cell ratio of 1:5 and co-cultured in EBM2 + 0.1% BSA for 2 hours. In contrast to the procedures described above the Jurkat cells were left unstimulated. Jurkat clones were labeled with PKH67 (see 2.5.2). Depending on the following experiments the co-cultured cells were fixed in PFA (paraformaldehyde) directly after trypsinization or harvested without fixation as described in 2.3.3. For fixation with PFA non-adherent Jurkat cells were removed and the ECs were washed with PBSdef. 4 ml of 1x trypsin-EDTA were added to each 10 cm plate and the cells were incubated until they detached from the dish and were then transferred directly into 15 ml falcon tubes containing 7 ml 10% PFA. The plates were washed with 3 ml PBSdef to harvest all residual cells. Those were again added to the tubes containing PFA.

The harvested (fixed or living) cells were centrifuged at 330 g for 5 min at RT and suspended in 100 µl 5% FCS in PBSdef. All harvesting steps and the following immunostaining for FACsorting were performed under sterile conditions. The first staining step was performed with mouse anti-human CD146-biotin (0.1 µl CD146-biotin antibody/$1x10^6$ cells) in 5% FCS in PBSdef. The pellet was resuspended in 100 µl and incubation took place at 4°C for 20 min. Afterwards 2 ml 5% FCS in PBSdef were added and the micron tubes were centrifuged at 3 x g for 3 min at RT. The second antibody solution contained streptavidin conjugated to PE-TexasRed (0.2 µl reagent/$1x10^6$ cells) and mouse anti-CD45-PC5 (5 µl CD45-PC5/$1x10^6$ cells) in 5% FCS in PBSdef. Again, the pellet was resuspended in 100 µl and incubation took place at 4°C for 20 min. After washing with 2 ml 5% FCS in PBSdef, centrifugation at 480 x g for 3 min at 4°C was performed and the cells were resuspended in 500 µl EGM2-MV w/o GFs and transferred into a snap cap tube. Cell sorting was performed in collaboration with the FACS Core Facility of the Medical University of Vienna headed by Andreas Spittler. 15 ml tubes were supplied with 3 ml EGM2-MV w/o GFs in which cells were sorted using a FACS Aria device (Becton Dickinson, Franklin Lakes, NJ, USA).

Materials

<u>Cell culture media and solutions:</u> see Materials 2.2

PKH67 Fluorescent Cell Linker (1 mM in ethanol)	(Sigma-Aldrich, St. Louis, MO, USA)
Diluent C	(Sigma-Aldrich, St. Louis, MO, USA)
Paraformaldehyde	(Sigma-Aldrich, St. Louis, MO, USA)

10% PFA in PBSdef

dissolved and heated to 65°C while stirring

heat reduction and addition of 1 to 2 ml 1 M NaOH dropwise until solution cleared

filtered and stored in aliquots at -20 °C

<u>Plastic equipment:</u> see Materials 2.2

10 cm cell culture dishes	(Corning Inc, NY, USA)
Snap cap tube	(Becton Dickinson, Franklin Lakes, NJ, USA)

<u>Antibodies:</u>

Mouse anti-human CD146-biotin	(Chemicon, Temecula, CA, USA (1:1000)
Mouse anti-human CD45-PC5 (clone J33)	(Immunotec Inc., Quebec, Canada (1:20)
Streptavidin-PE-TexasRed	(Becton Dickinson, Franklin Lakes, NJ, USA (1:500)

2.9 Western blot

2.9.1 Preparation of protein extracts

Sorted, PFA-fixed cells were centrifuged at 480 x g for 3 min at RT. The supernatant was removed and the pellet was resuspended in 40 μl SDS lysis buffer containing a protease inhibitor cocktail. The samples were heated to 95°C for 5 min, placed on ice and briefly centrifuged. The lysates were then sonicated (30% sonication and 70% break per second) for 1 min and centrifuged for 10 min at 10000 g and 4°C. The supernatant, containing the proteins of the whole cells, was transferred into a new 0.5 ml reaction tube and snap frozen in liquid N_2. Samples were stored at -20°C. An aliquot for protein quantitation by BCA test was frozen separately.

Materials

Cell culture media and solutions:

cOmplete Mini: protease inhibitor tablets	(Roche Pharma AG, Basel, Switzerland)
10x protease inhibitor cocktail:	cOmplete Mini protease inhibitor tablet dissolved in 1 ml of SDS lysis buffer

SDS lysis buffer:

100 mM Tris-HCI

1% SDS

pH 9.5

Note: The SDS lysis buffer was freshly supplemented 1:10 with the 10x proteinase inhibitor cocktail prior to use.

Equipment:

Sonication device: UIS250L Sonicator with Sonotrode LTS24d10.4L2 and electronic timer T1 (Hielscher, Teltow, Germany)

2.9.2 Protein measurement by BCA test

To determine the protein concentration of the samples a BCA (bicinchoninic acid) test was performed. Samples were thawed and pre-diluted 1:2 with ddH_2O (double distilled water). BSA standards were prepared according to the manufacturer's instructions. 20 µl of BCA standards (2000, 1500, 1000, 750, 500, 250, 125, 25 or 0 µg/ml protein) or pre-diluted samples of cell extracts were mixed in 1.5 ml reaction tubes with 400 µl working reagent (Solution A : Solution B = 50:1) and incubated at 37°C for 30 min. Afterwards samples were centrifuged briefly and duplets of 200 µl were pipetted into a 96-well plate with flat bottom. Protein concentrations were measured photometrically at 562 nm using a Varioskan Flash Multimode Reader (Thermo Scientific, Waltham, MA, USA). A standard curve was generated and the protein concentrations of the samples were calculated.

Materials

Cell culture media and solutions:

BCA Protein Assay Kit (Pierce Biotechnology, Rockford, IL, USA) containing:

BCA Reagent A

BCA Reagent B

Albumin standard (2 mg/ml)

PBSdef (Ca^{2+} / Mg^{2+}-free)   (PAA, Pasching, Austria)

Plastic equipment:

TPP® 96 well plate, flat bottom

1.5 ml reaction tube   (Greiner Bio-One)

2.9.3 Sodium dodecyl sulfate polyacrylamide gel electrophoresis

Protein samples were subsequently subjected to sodium dodecyl sulfate polyacrylamide gel electrophoresis (SDS/PAGE) to separate proteins according to molecular weight. As a first step the running gel was prepared (according to tab. 4) to obtain a 10% polyacrylamide gel. Ammonium persulfate (APS) and N,N,N',N'-tetramethylethylenediamine (TEMED) were added as the last components to start and catalyze the acrylamide polymerization. After mixing the solution it was poured between a glass and ceramic plate separated by 0.75 mm spacers. Glass, plate and spacer were fixed in a Hoefer SE245 Mighty Small Dual Gel Caster. 300 µl of n-butanol were added on top to obtain a smooth gel surface. Polymerization proceeded for about 60 min. Afterwards n-butanol was removed from the surface and the plate was dried using small pieces of filter paper. Now the stacking gel was mixed according to tab. 5 to obtain a 4.7 % polyacrylamide gel. After adding the solution on top of the running gel a comb for 10 x 5 mm sample slots was adjusted. A second polymerization step of about 1 h followed. As a last step the gel together with the two plates and the spacer (the comb was removed after polymerization) were transferred to a Hoefer SE250/SE260 Mighty Small electrophoresis chamber. About 300 ml of electrophoresis buffer (1x TANK buffer) were added. The gel slots were rinsed with the buffer and samples (as well as protein marker) were loaded. Samples were diluted to 2 µg protein in 10 µl SDS lysis buffer according to the BCA test results. 2 µl 5x SLAB loading buffer (including DTT 1:10) were added and the samples were heated to

95°C for 5 min. After a short centrifugation, 10 µl of the samples were loaded in the slots of the gel. Furthermore, 3 µl of a biotinylated protein ladder were heated to 95°C for 5 min and loaded as well as 5 µl of a Kaleidoscope prestained protein standard. 15 mA per gel was applied to perform the electrophoresis.

Materials

AA/Bis-solution 40%	3.0 ml
4 x running gel buffer	3.0 ml
ddH$_2$O	6.0 ml
APS 40%	16 µl
TEMED	8 µl

Tab. 4: Components for a 10% resolving gel

AA/Bis-solution 40%	0,7 ml
4 x running gel buffer	1,5 ml
ddH$_2$O	3,8 ml
APS 40%	16 µl
TEMED	8 µl

Tab. 5: Components for a 4.7% stacking gel

Materials

<u>Reagents:</u>

TEMED: N,N,N',N'-tetramethylethylenediamine   (Bio-Rad)

n-Butanol   (Merck KGaA, Darmstadt, Germany)

Biotinylated Protein Ladder Detection Pack: biotinylated protein ladder in premixed format and HRP (horse radish peroxidase)-linked anti-biotin antibody (Cell Signaling, Beverly, MA, USA)

Kaleidoscope prestained standard   (Bio-Rad)

AA/Bis-solution 40%: acrylamide, bisacrylamide 40% solution 37.5/1 (GERBU Biotechnik GmbH, Heidelberg, Germany)

Tris: tris(hydroxymethyl)aminomethane   (Merck KGaA)

SDS: sodium dodecyl sulfate   (BioRad)

Glycine   (Merck KGaA)

Glycerol   (Sigma-Aldrich)

APS: ammonium persulfate   (Merck KGaA)

ß-mercaptoethanol   (Sigma-Aldrich)

37% HCl: hydrochloric acid (AnalR Normapur BDH Prolabo, VWR International GmbH, Darmstadt, Germany)

0.5% bromophenol blue   (Serva, Heidelberg, Germany)

DTT: dithiothreitol   (Sigma Aldrich)

<u>Buffers and Solutions:</u>

4 x running gel buffer:

1.5 M Tris

0.4% SDS

pH 8.8 (adjusted with HCl)

stored at 4°C

4 x stacking gel buffer:

0.5 M Tris

0.4% SDS

pH 6.8 (adjusted with HCl)

stored at 4°C

10 x TANK buffer:

25 mM Tris

192 mM glycine

0.1% SDS

stored at RT

1 x TANK buffer (working solution):

10 x TANK buffer diluted 1:10 with ddH2O

5x SLAB buffer:

150 mM Tris

5% SDS

25% glycerol

0.5% bromophenol blue

+/- 11.5% β-SH

pH 6.8 (adjusted with HCl)

aliquots stored at -20°C

40% APS:

 0.8 g ammonium persulfate

ddH$_2$O to 2 ml

aliquots stored at -20°C

4 M DTT:

0.3 g DTT

ddH$_2$O to 500 µl

aliquots stored at -20°C

Plastic equipment:

Hoefer Mighty Small system for gel preparation and electrophoresis:

Hoefer Mighty Small Dual Gel Caster SE245 and Hoefer Mighty Small SE250/SE260 mini-vertical electrophoresis unit, including glass and ceramic plates, spacers, combs (Hoefer Inc., Holliston, MA, USA)

Amersham™ ECL™ Gel Box	(GE Healthcare, Buckinghamshire, United Kingdom)
4-12% Amersham ECL gradient gel	(GE Healthcare, Buckinghamshire, United Kingdom)
Thermomixer Comfort	(Eppendorf)
PowerPac Basic power supply	(Bio-Rad Laboratories, Inc., Hercules, CA, USA)
1.5 ml reaction tube	(Greiner Bio-One)
Polystyrene Round Bottom Test Tube	(Becton Dickinson, Franklin Lakes, NJ, USA)

2.9.4 Immunoblotting

Following SDS/PAGE separation proteins were transferred to a membrane for subsequent immunoblotting. Thus, a 6 x 8 cm poly(vinylidene fluoride) membrane piece was cut and activated with methanol for 15 seconds. The membrane was washed with ddH_2O for 2 minutes and equilibrated with semi-dry blotting buffer for 5 min. Also two pieces of BioRad blotting paper with the same size of 6 x 8 cm were equilibrated with semi-dry blotting buffer. After the electrophoresis a blotting sandwich was assembled in the following order: Whatman paper, protein gel (separated from glass and ceramic plates; stacking gel was removed as well), membrane and Whatman paper. The sandwich was placed in a Hoefer Scientific Semiphor Electrophoresis Blotter TE-70 #11 and semidry blotting was performed with 39 mA for 1 h. After blotting the membrane was transferred into a 50 ml reaction tube (with skirt) and blocked with 5 ml freshly prepared blocking solution over night on a tuber roller at 4°C. On the next day the primary antibody directed against ERK 1/2 or pERK 1/2 was diluted 1:1000 in 3 ml blocking solution and added for 1 h. Incubation of the membrane took place at 4°C while rolling on a roller device. Before adding the secondary antibody solution containing anti-biotin-HRP (1:100.000) and goat anti-rabbit HRP (1:5000) in 3 ml blocking solution the membrane was rinsed three times with wash buffer for 5 min each at RT. The incubation with secondary antibody solution proceeded for 1 h at 4°C on a roller device and afterwards the membrane was washed again three times. The membrane was then transferred onto a plastic wrap (transparent sheet protector) and 500 μl of the HRP chemiluminescence substrate (previously prepared as a 1:1 mix) were added and incubated for 5 min. Air bubbles were been removed. The membrane was briefly dried and was immediately analyzed by G-BOX using GeneSnap software by SynGene or was exposed to Amersham Hyperfilm™ ECL.

Materials

Reagents:

Lumigen® TMA-6 Chemiluminescent Reagent   (Lumigen, Inc., Southfield, Michigan, USA)

SDS: sodium dodecyl sulfate   (BioRad)

PBSdef (Ca^{2+} / Mg^{2+}-free)   (PAA, Pasching, Austria)

Ethanol absolute: AnalR NORMAPUR   (VWR International GmbH)

Methanol   (Merck KGaA)

Tris: tris(hydroxymethyl)aminomethane   (Merck KGaA)

Glycine   (Merck KGaA)

Blotting-Grade Blocker: nonfat dry milk   (BioRad)

Tween 20: polyoxyethylenesorbitan monolaurate   (Sigma-Aldrich)

Primary antibodies:

Rabbit anti-human p44/42 MAPK (ERK1/2) (1:1000)   (Cell Signaling)

Rabbit anti-human phospho-p44/42 MAPK (pERK1/2) (1:1000)   (Cell Signaling)

Secondary antibodies:

Goat α-rabbit IgG-HRP-conjugate (1:100.000)   (Santa Cruz Biotechnology, CA, USA)

anti-biotin-HRP-conjugate (1:5000)   (Cell Signaling)

Buffers and Solutions:

Semi-dry blotting buffer:

25 mM Tris

192 mM glycine

0.1% SDS

20% methanol

pH should be at 8.1-8.4

stored at RT

Blocking solution:

5 g non-fat milk powder

in 50 ml wash buffer

filtered

Wash buffer:

0.05% Tween 20

in PBSdef

<u>Equipment:</u>

Hoefer Scientific Semiphor Electrophoresis Blotter TE-70 #11 (Hoefer Inc., Holliston, MA, USA)

G-Box   (SynGene, Cambridge, United Kingdom)

Roller device: RM-5 30V CAT   (Ingenieurbüro CAT M. Zipperer GmbH, Staufen, Germany)

Immobilon®-P poly(vinylidene fluoride) transfer membrane   (Millipore, Merck KGaA)

BioRad Extra Thick Blot Paper   (BioRad)

50 ml reaction tubes with skirt   (Sarstedt AG)

Amersham Hyperfilm™ ECL   (GE Healthcare, Buckinghamshire, United Kingdom)

2.10 Confocal laser scanning microscopy

2.10.1 Immunostaining

Confocal laser scanning microscopy (CLSM) was applied to visualize intercellular EGFP-Ras transfer to recipient endothelial cells. As a first step glass slides and glass cover slips were rinsed in 96% ethanol and dried afterwards. Jurkat cells and ECs were prepared as described in 2.4. After a co-culture experiment of 2 h, the cells were stained for confocal laser scanning microscopy as follows: ECs and attached Jurkat cells were harvested (see 2.3.3) and transferred into micron tubes and centrifuged at 480 x g for 3 min at room temperature. The cell pellet was resuspended in 1 ml PBSdef containing 1 µl of brilliant violet dye (LIVE/DEAD Fixable Violet Dead Cell Stain Kit). After 30 min of incubation at RT in the dark the micron tubes were centrifuged again and the pellet was washed with 1 ml PBSdef. The first antibody solution contained mouse anti-human CD146-biotin (1:1000) in 5% FCS in PBSdef. The pellet was resuspended in 100 µl and incubated at 4°C for 20 min. Afterwards 1

ml 5% FCS in PBSdef was added and the micron tubes were centrifuged at 480 x g for 3 min at 4°C. The second antibody solution contained goat anti-mouse Alexa Fluor® 633 (1:1000) in 5% FCS in PBSdef. Again the pellet was resuspended in 100 µl and incubated at 4°C for 20 min. The pellet was resuspended in 500 µl 5% FCS in PBSdef and distributed to two micron tubes for two different approaches: surface and intracellular EGFP staining.

For the surface staining the cells were centrifuged and the pellet was resuspended in the third antibody solution containing rabbit anti-EGFP IgG (1:100) in 5% FCS in PBSdef. Incubation took place at 4°C for 20 min. Afterwards 1 ml 5% FCS in PBSdef was added and the micron tubes were centrifuged at 480 x g for 3 min at RT. The last antibody solution contained goat anti-rabbit Alexa Fluor® 546 (1:1000) in 5% FCS in PBSdef. Incubation was performed at 4°C for 20 min. Afterwards 1 ml 5% FCS in PBSdef was added and the micron tubes were centrifuged at 480 x g for 3 min at RT. The pellet was now resuspended in 15 µl CLSM buffer and was spread on the microscope glass slide. After the suspension on the microscope glass slide had dried, a small drop of Fluoromount-G® was added and a glass cover slip was put on top of the mounting medium and pressed carefully onto the glass slide.

For intracellular staining the cells were centrifuged and fixed with 100 µl of Fixation Buffer (Buffer 1; Intraprep Permeabilization Kit). After adding 100 µl Buffer 1 cells were vortexed thoroughly. After 15 min of incubation in the dark at RT, 1 ml PBSdef was added and the micron tubes were centrifuged. For intracellular staining the antibodies were diluted in a solution of PBSdef and Permeabilization Buffer (Buffer 2; Intraprep Permeabilization Kit) (1:1). Then, the third antibody solution containing rabbit anti-EGFP IgG (1:100) and the fourth antibody solution containing goat anti-rabbit Alexa Fluor® 546 (1:1000) were sequentially applied as follows. After 5 min of incubation with the third antibody solution (100 µl) the micron tubes were tapped by finger and 15 additional minutes of incubation followed. 1 ml PBSdef was added and after centrifugation the last (fourth) antibody solution (100 µl) was added. After 5 min of incubation the micron tubes were again tapped and 15 further minutes of incubation at RT followed. The last washing step was performed with 1 ml PBSdef and subsequent centrifugation. The pellet was now resuspended in 15 µl CLSM buffer and was spread on the microscope glass slide. After drying, the cells were mounted with Fluoromount-G as described above. Samples were examined with a laser scanning microscope LSM 780 (Carl Zeiss Microscopy, Thornwood, NY, USA).

Materials

Media and Solutions:

CLSM Buffer:

1.5% BSA + 0.1% NaN_3 in PBSdef

sterile filtered (0.22 µm filter)

stored at 4°C

Intraprep Permeabilization Reagent	(Beckman Coulter, Brea, CA, USA)
LIVE/DEAD Fixable Violet Dead Cell Stain Kit	(Invitrogen, Carlsbad, CA, USA)

Primary antibodies:

Mouse anti-human CD146-biotin (1:1000)	(Invitrogen, Carlsbad, CA, USA)
Rabbit anti-EGFP IgG (1:100)	(Invitrogen, Carlsbad, CA, USA)

Secondary antibodies:

Alexa Fluor® 546 goat anti-rabbit IgG (H+L), 2 mg/ml, A-11010 (1:1000)

Alexa Fluor® 633 goat anti-mouse IgG (H+L), 2 mg/ml, A21053 (1:1000)

(all from Invitrogen, Carlsbad, CA, USA)

Equipment:

Zeiss LSM 780 confocal laser scanning microscope (Carl Zeiss Microscopy, Thornwood, NY, USA)

6-well tissue culture (TC)-treated microplates (30 mm wells)

 (TPP, Trasadingen, Switzerland)

Reaction tubes 1.5 ml (Greiner Bio-One, Frickenhausen, Germany)

Glass cover slips (Marienfeld-Superior, Lauda Königshofen, Germany)

StarFrost® adhesive silane-treated glass slides (Knittel, Braunschweig, Germany)

Fluoromount G® mounting medium (Southern Biotech, Chicago, IL)

3. RESULTS

3.1 Flow cytometric detection of EGFP-Ras transfer from lymphoma cells to ECs

In continuation of the preliminary work conducted by Katrin Gitschtaler [74] this thesis project confirmed the EGFP-Ras transfer from stably transfected Jurkat clones to endothelial cells. After performing trans-endothelial migration assays or co-culture experiments (as described in Materials and Methods) cells were analyzed via flow cytometry and data were evaluated using Kaluza Analysis Software 1.3 (Beckman Coulter®).

Endothelial cells were stained for CD146 (melanoma cell adhesion molecule or MCAM) and Jurkat cells for CD45 (protein tyrosine phosphatase). These two surface markers enabled the distinction of the two populations (Fig. 9A). By including a live-dead cell stain in the immunolabeling procedure only living ECs (Fig. 9B) were analyzed within the endothelial cell gate for EGFP antigen (Fig. 9C/9D). This was achieved by setting the CD146 PE-TexasRed signal on the x-axis and the EGFP signal, which was detected via rabbit anti-EGFP and goat anti-rabbit Alexa Fluor® 700, on the y-axis.

Although the Ras protein was fused to an EGFP molecule, the intrinsic EGFP fluorescence was not strong enough to efficiently detect ECs with transferred EGFP-Ras protein due to the high autofluorescence of the ECs in the green fluorescence channel. Thus, EGFP-Ras molecules were detected with anti-EGFP antibody and a secondary reagent fluorescing in the far-red channel (Alexa Fluor® 700). Endothelial cells co-cultured with parental Jurkat cells served as a negative control and gates were set accordingly (Fig. 9C+D).
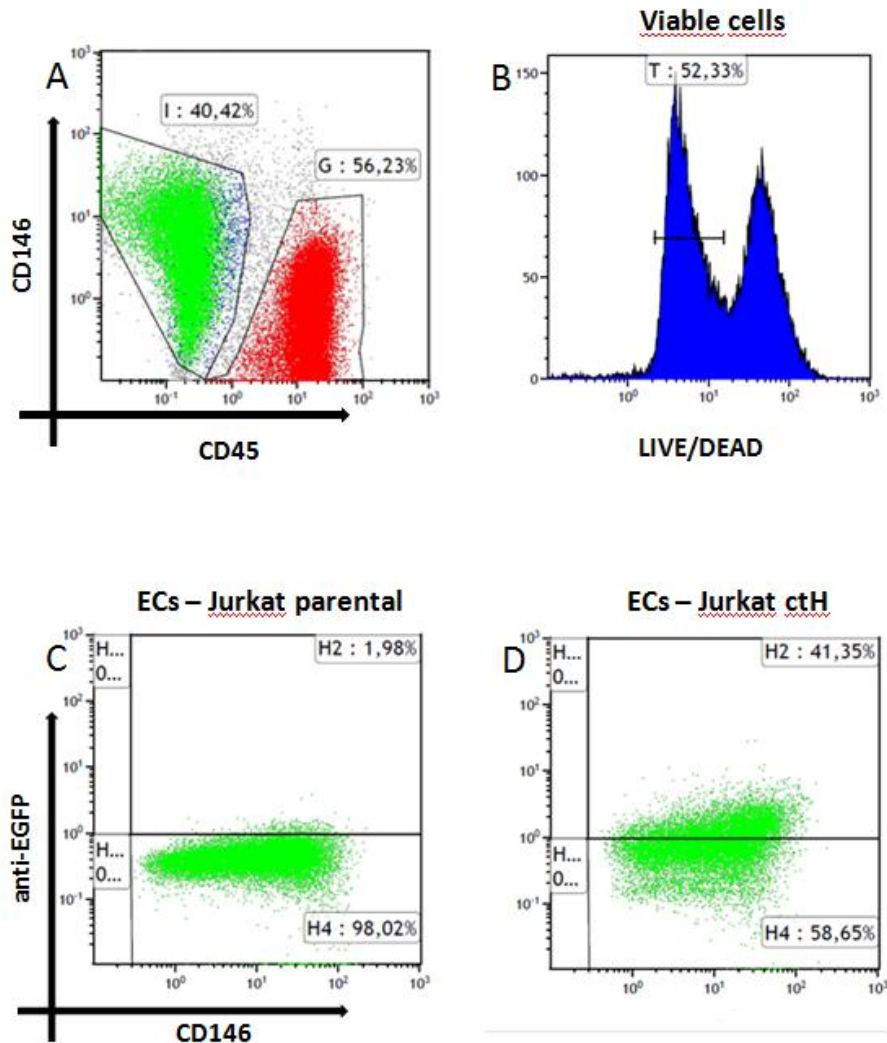
Fig. 9: Gating strategy for flow cytometric detection of EGFP-Ras transfer from lymphoma cells to ECs:

A co-culture experiment of ECs with parental Jurkat cells or the ctH clone (cell ratio of 1:5) was performed for 4 h. Cells were harvested, stained and analyzed via flow cytometry. (A) CD146$^+$ ECs (green) and CD45$^+$ Jurkat cells (red) were separated in the first gating step. (B) Viable ECs were distinguished from dead cells (positive for LIVE/DEAD Fixable Violet Dead Cell Stain), gated and selectively analyzed in the following steps. (C) The negative gate for EGFP detection was set to 98% of viable CD146$^+$ ECs co-cultured with the parental Jurkat cells. (D) EGFP-Ras transfer was reflected by the percentage of double-positive (CD146$^+$ and anti-EGFP$^+$) ECs after 4 h of co-culture with the Jurkat ctH clone.

3.2 Impact of acceptor to donor cell ratio and type of EGFP-Ras construct on the transfer efficiency of EGFP-Ras molecules

The next set of experiments was designed to test for the best ratio of ECs and Jurkat cells to achieve maximal transfer of EGFP-Ras. The experiments involved the co-culture of ECs with either parental Jurkat cells or Jurkat clones expressing different EGFP-Ras variants (compare Fig. 8) in a 1:1, 1:5 or 1:10 ratio. Furthermore, detection of transferred EGFP-Ras by the intrinsic green fluorescence of the EGFP molecule was compared to EC permeabilization and

52

anti-EGFP antibody staining with an Alexa Fluor® 700 conjugate. In both cases (EGFP and anti-EGFP signal) the negative gate of ECs co-cultured with parental Jurkat cells was set to 98% (compare Fig. 9C).

With the exception of the C3 control clone, detection of EGFP-Ras transfer from Jurkat clones (ctH, H12V and K12V) to ECs was consistently more sensitive when using anti-EGFP antibody than when monitoring intrinsic EGFP fluorescence (compare Fig. 10A to 10B). The Jurkat C3 clone expressed EGFP without Ras fusion and was included as a negative control, since EGFP expression in the absence of Ras sequences was primarily cytoplasmic and hence unlikely to be transferred by membrane-mediated protein exchange. Interestingly, the signal of transferred cytoplasmic EGFP from the C3 clone was higher in the case of EGFP detection (max. 9% EGFP$^+$ ECs) than for anti-EGFP detection (max. 6% EGFP$^+$ ECs). Furthermore, transfer of cytoplasmic EGFP from Jurkat C3 cells onto ECs as detected by EGFP fluorescence was increasing when the Jurkat to EC ratio was elevated. Such a dose-dependent increase of cytoplasmic EGFP transfer could not be detected with anti-EGFP staining of ECs.

Comparing the transfer of membrane-located EGFP-Ras fusion constructs (ctH, H12V and K12V) at different acceptor to donor cell ratios, a distinct dose dependence was observed. At a ratio of 1:1 little transfer was detectable. But by executing the experiment with the higher ratios of 1:5 or 1:10 EGFP-Ras exchange was evident. For instance, when analyzing co-culture experiments with the EGFP-ctH Jurkat clone, 10% of EC were positive for the anti-EGFP signal at the lowest acceptor to donor ratio of 1:1. When the ratio was increased to 1:5 or 1:10 approximately 25% of ECs were positive for EGFP-ctH transfer. Of note, there was no difference in transfer efficiency between the ratios of 1:5 and 1:10. Compared to the EGFP-ctH clone, protein transfer from the EGFP-H12V clone was lower (7-14% EGFP$^+$ ECs) as monitored by anti-EGFP antibody. Again, the highest transfer could be observed for the acceptor to donor ratio of 1:5 which could not be further raised by the 1:10 setting. The transfer efficiency for the EGFP-K12V Ras molecule from Jurkat cells to ECs was modest (max. 7% when detected by anti-EGFP antibody) and comparable for 1:5 and 1:10 cell ratios.

Thus, using the flow cytometric strategy and data analysis described in 3.1 we found that the efficiency of EGFP-Ras transfer from lymphoma cells to ECs depended on the one hand on the ratio of ECs to Jurkat cells and on the other hand on the EGFP-Ras fusion construct that was expressed by the Jurkat cells. In general, transfer detection by anti-EGFP antibody was more sensitive than measuring intrinsic EGFP fluorescence.
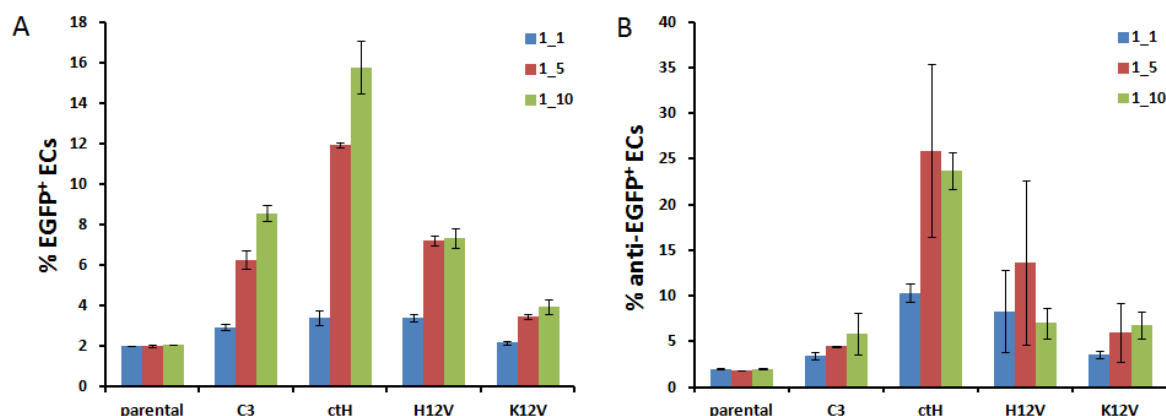
Fig. 10: Impact of EC to Jurkat cell ratio and of EGFP-Ras construct on transfer efficiency:

Endothelial cells were co-cultured with parental Jurkat cells or Jurkat cells clones expressing EGFP-Ras variants (C3, ctH, H12V and K12V) in three different acceptor to donor cell ratios (1:1, 1:5 and 1:10) for 4 h. ECs were harvested, stained and analyzed via flow cytometry. (A) ECs were stained for CD146 and the transfer of the EGFP-Ras fusion protein was detected via the intrinsic EGFP fluorescence signal. (B) ECs were stained for CD146, permeabilized and incubated with rabbit anti-EGFP followed by goat anti-rabbit Alexa Fluor® 700. The anti-EGFP signal was used to detect EGFP+ ECs. Mean values and standard deviations from 2 independent experiments are shown.

3.3 Time course of EGFP-Ras transfer from donor to acceptor cell

Trogocytosis is described as being fast, efficient and requires only a few minutes of cell contact [69]. The next experiment sets the focus on the transfer rate of the EGFP-Ras fusion molecules (ctH, H12V and K12V) between Jurkat cells and ECs. Therefore, we performed co-culture experiments with an EC to Jurkat ratio of 1:5. The duration of the co-culture was in a range from 15 min to 4 h. Afterwards cells were harvested and analyzed by flow cytometry. Again, the anti-EGFP signal was used for evaluation of EGFP+ ECs.

After co-culturing ECs with Jurkat ctH cells a rapid transfer was observed. After 15 min 33% of ECs were positive for EGFP. The following time points did not show a substantial increase, but the maximum was reached after 2 h with 39% of EGFP+ ECs. However, the first time point at 15 min showed a very high interassay standard deviation. With increasing duration of the co-culture the standard deviation decreased. Comparable results were observed for the H12V clone. After 15 min of co-culture 27% of ECs presented positive for the EGFP-Ras molecule. After 30 min the maximum of 30% of EGFP+ ECs was reached and interestingly after 4 h only 17% of the ECs were detected positive for EGFP. Experiments with the Jurkat EGFP-Ras K12V clone yielded a very low transfer efficiency (also reported in 3.2). Only 8.5% of ECs were detected positive for the EGFP-Ras K12V molecule after 15 min and the maximum of EGFP+ ECs was reached after 2 h with about 13%. When combining the

results of the three clones, the highest transfer efficiency was observed after 1-2 h of co-culture with endothelial cells.
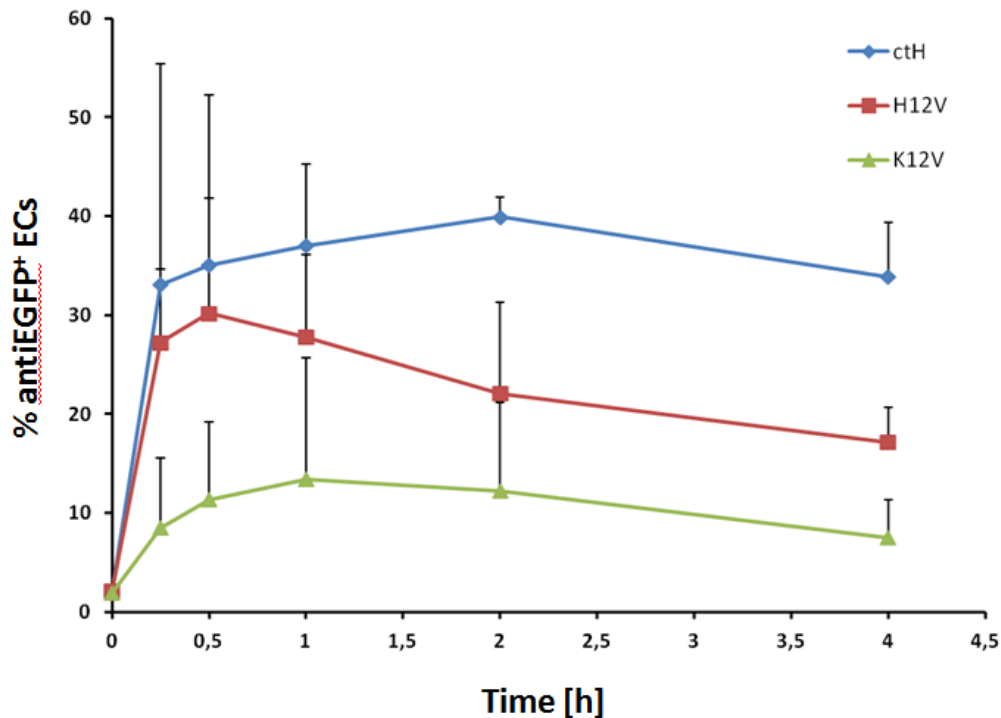
Fig. 11: Time course of EGFP-Ras transfer:

Co-culture of ECs and Jurkat cells or clones for 15 min, 30 min, 1, 2 or 4 h at a cell ratio of 1:5 followed by flow cytometric detection of transferred EGFP-Ras. ECs were detected by CD146 and further stained with rabbit anti-EGFP followed by goat anti-rabbit Alexa Fluor® 700. Mean values and standard deviations from 2 independent experiments are shown.

3.4. Localization of the transferred EGFP-Ras in the recipient cell

In the previous experiments we could show, that different EGFP-Ras constructs were rapidly transferred from Jurkat cells onto interacting ECs. Not only the transfer itself and its rate are of interest but also the localization of the transferred Ras molecule, as the proper intracellular membrane orientation would allow for functional Ras signaling.

To address this question we performed co-culture experiments with an EC to Jurkat ratio of 1:5. The duration of the co-culture was 4 h. Afterwards cells were harvested and analyzed by flow cytometry and additionally with confocal laser scanning microscopy. In both cases the cells were stained with antibodies against EGFP. To be able to distinguish between surface-

bound and intracellular EGFP, immunostaining was performed without or with cell permeabilization, respectively.

Thus, when the cells were not permeabilized, the anti-EGFP antibody could not enter the cell and therefore only bound to surface EGFP molecules. In contrast, when the cells were permeabilized the antibody was able to permeate the cell membrane and bind to intracellular EGFP-Ras fusion proteins. Fig. 12 shows anti-EGFP^{+} ECs for permeabilized and non-permeabilized preparations. Very little EGFP (generally below 5%) was detected with surface staining of endothelial cells. The results of the intracellular staining of the ECs were as follows: After co-culturing ECs with Jurkat EGFP-C3 cells, only 6% of ECs were EGFP positive. Co-culturing ECs with the Jurkat ctH clone resulted in 43% EGFP positive ECs. For the H12V construct 13% and for the K12V construct 7% of ECs were detected positive for EGFP when cells had been permeabilized. These results indicate an intracellular localization of the transferred EGFP molecules when connected to Ras sequences.
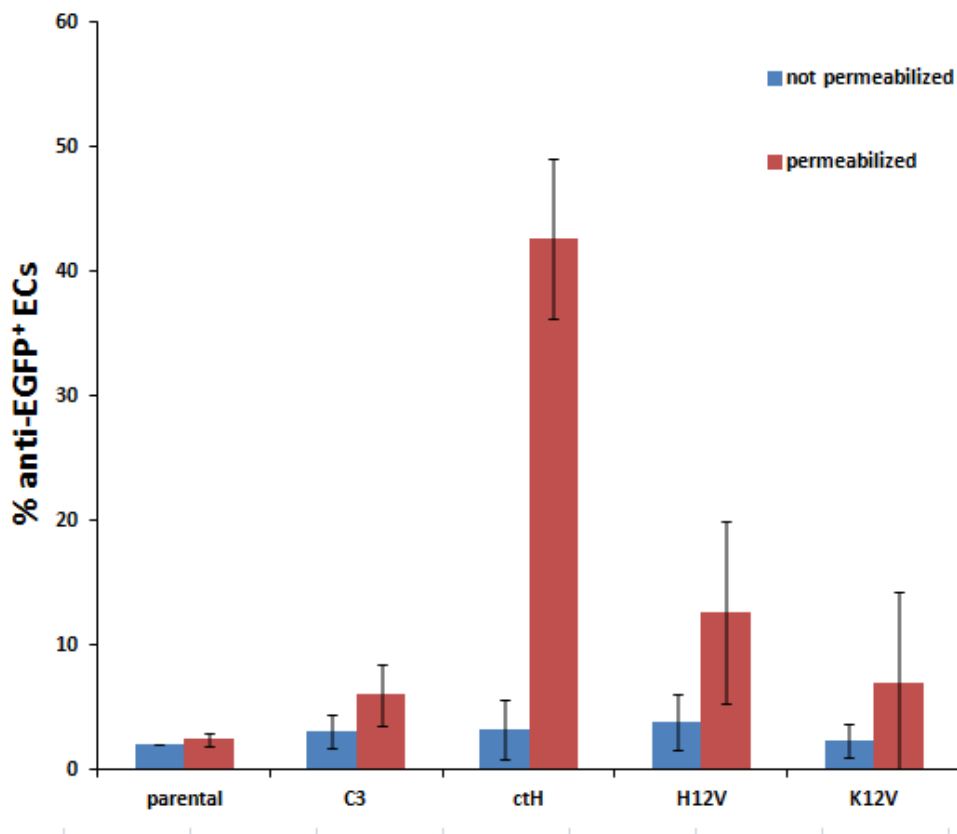
Fig. 12: Intracellular versus surface detection of transferred EGFP-Ras by flow cytometry:

After 4 h of co-culture with parental Jurkat cells or the four Jurkat cells clones (C3, ctH, H12V and K12V) ECs were stained for EGFP-Ras transfer with rabbit anti-EGFP antibody to discriminate between surface-bound (non-permeabilized ECs) and intracellularly oriented (permeabilized ECs) EGFP-Ras molecules. Cells were analyzed by flow cytometry. Mean values and standard deviations from 2 independent experiments are shown.

After establishing that the transferred EGFP-Ras molecule was mainly located at the inside of the recipient cell the subcellular localization remained to be determined. Therefore, CLSM was used for further analysis. As mentioned above, cell permeabilization and the anti-EGFP antibody were applied to discriminate between surface bound and intracellular EGFP molecules.

Fig. 13 depicts CD146 expression in white which distinguishes CD146$^+$ ECs from CD146$^-$ Jurkat cells. EGFP expression is represented by green color for the intrinsic green fluorescence signal of the protein, and is further detected by anti-EGFP antibody binding as shown in red. A yellow signal represents the concomitant detection of EGFP by intrinsic fluorescence and anti-EGFP antibody as illustrated by channel overlay. While the Jurkat C3 control clone shows EGFP expression in the cytosol, the EGFP molecules fused to Ras sequences (ctH, H12V, K12V) are predominantly located at the plasma membrane of Jurkat clones. Protein transfer is only detected for EGFP-Ras fusion molecules (but not for the EGFP control protein) and is restricted to focal points of the endothelial cell membrane as illustrated by bright green and red dots. While green signals (intrinsic EGFP fluorescence) are independent of cell permeabilization, the red staining (by anti-EGFP antibody) is only observed for permeabilized ECs. In summary, this supports the notion that membrane-anchored EGFP (fused to Ras sequences) is transferred from Jurkat donor cells onto EC membranes in the appropriate inner-membrane orientation.

A

	CD146	EGFP	antiEGFP	Merge
parental				
C3				
ctH				
H12V				
K12V				
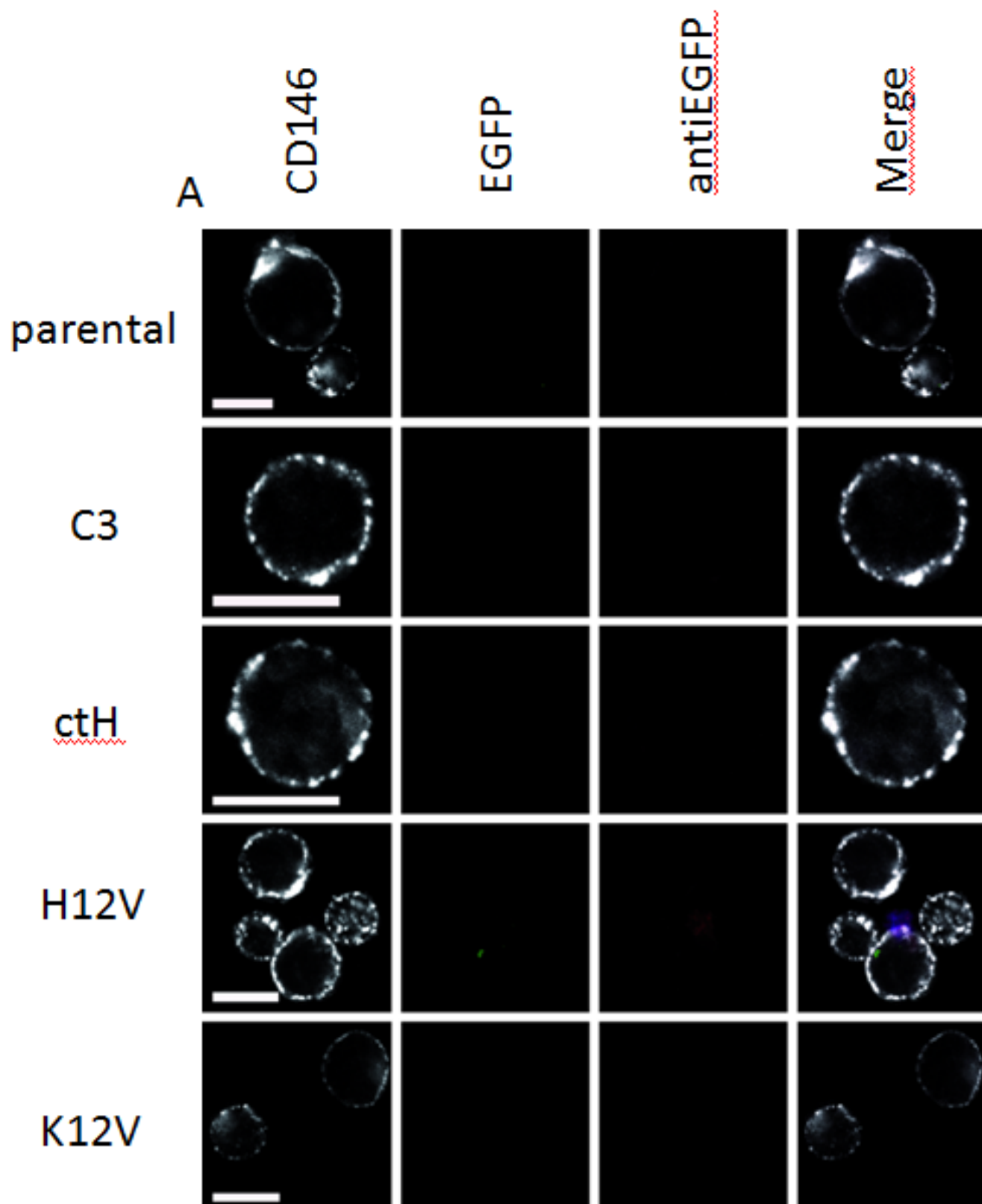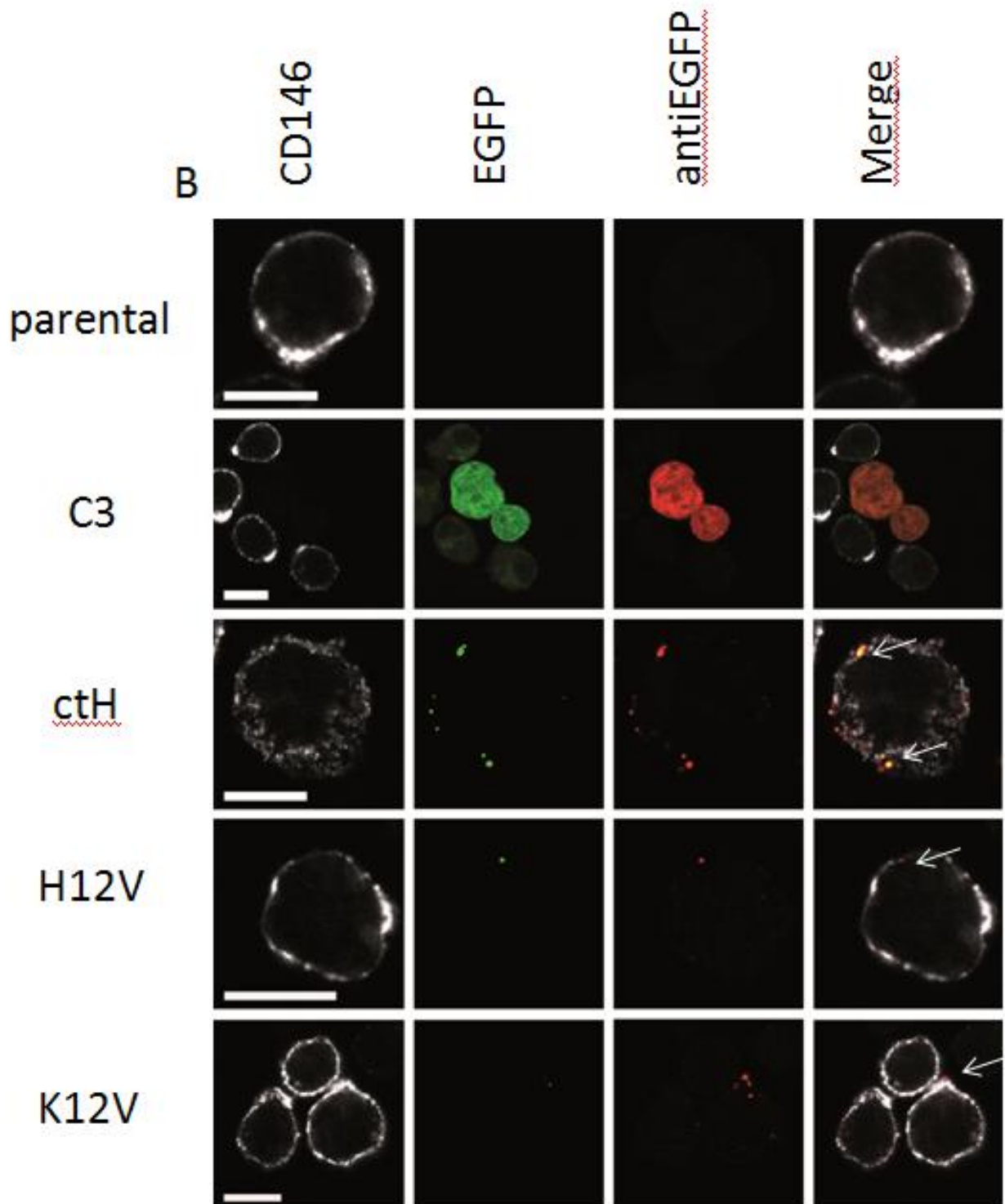
Fig. 13: Subcellular localization of transferred EGFP-Ras using confocal laser scanning microscopy:

Co-culture of parental Jurkat cells or the four Jurkat cells clones (C3, ctH, H12V and K12V) with ECs was performed for 4 h. Cells were harvested and immunostained by CD146 as well as EGFP antibodies with (B) or without (A) cell permeabilization. Confocal laser scanning microscopy was applied to visualize CD146$^+$ ECs (white), intrinsic EGFP fluorescence (green) and anti-EGFP antibody signals (red). The overlay illustrates the concomitant detection of EGFP by intrinsic fluorescence and antibody by yellow color (indicated by white arrows). Scale bar: 10 μm.

3.5 EGFP-Ras retention after transfer

The next aim was to evaluate the half-life of the transferred EGFP-Ras molecule in endothelial cells. This information was of particular interest for the potential function and signaling capacity of the transferred molecules in the recipient cells.

The experiment was performed as follows: A co-culture (2 h) with an EC to Jurkat ratio of 1:5 was performed. The Jurkat cells were removed from the adherent EC monolayer by excessive washing to prevent further exchange of EGFP-Ras molecules. ECs were further kept in culture for different time periods (0, 24, 48 and 72 h) and subsequently analyzed by flow cytometry for EGFP-Ras retention.

Directly after 2 h of co-culture 28% of ECs were detected positive for EGFP-ctH using the anti-EGFP signal. At the next time points of 24, 48 and 72 h the percentage of EGFP$^+$ ECs decreased approximately by half to 12%, 7% and 2%, respectively (Fig. 14). A comparable result was achieved when monitoring the intrinsic EGFP signal. The percentage of EGFP$^+$ ECs was reduced by approximately half with every 24 h from 13% to 7% to 3.5% (data not shown). After co-culture of Jurkat H12V or K12V clones with ECs, only 10% and 6% of ECs were detected positive for EGFP at the 0 h time point, respectively. In both cases the number of EGFP$^+$ ECs diminished very rapidly. After 48 h almost none ECs (3% for H12V and 2% for K12V) were detected positive. ECs co-cultured with parental Jurkat cells served as negative control.

Fig. 14: EC retention of EGFP-Ras molecules after transfer from Jurkat cells onto ECs:

Parental Jurkat cells or Jurkat clones ctH (A), H12V (B) and K12V (C) were co-cultured with ECs in a ratio of 1:5 for 2 h. Thereafter, Jurkat cells were removed by excessive washing and EC culture was continued. ECs were harvested, stained and analyzed for EGFP-Ras molecules via flow cytometry after 0 h, 24 h, 48 h and 72 h. Data represent mean and SD of two independent

3.6 Transfer of membrane patches from Jurkat lymphoma to endothelial cells

When first reported for B- and T-cells, the intercellular transfer of EGFP-Ras molecules was found to be mediated by trogocytosis [65]. Therefore, the potential transfer mechanism of trogocytosis was also addressed in our experimental setting. Trogocytosis is described as the cellular exchange of whole membrane patches and of the molecules that are integrated into the membrane. The membrane transfer is commonly visualized by membrane dyes. The cell tracker PKH67 has a long aliphatic carbon tail and is used for cell membrane labeling. Its fluorescence has been described to be similar to EGFP, i.e., it is monitored in the same (green) channel as EGFP in flow cytometry (Fig. 15 B-E) [76].

Since membrane exchange between cells may occur by cell contact as for trogocytosis but may also be mediated by released vesicles such as exosomes, we used three different settings to investigate the transfer of PKH67 from Jurkat cells onto ECs: We performed direct 4 h co-cultures as opposed to transwell experiments where the co-cultured cells were separated by a membrane with 0.1 µm pore size. Furthermore, we harvested the supernatant of PKH67 labeled Jurkat cells and added it onto EC cultures for 4 hours.

After culturing PKH67 stained Jurkat cells in direct cell contact with ECs for 4 h, 55% of ECs were positive for the membrane dye PKH67 (Fig. 15C). Separating the PKH67 stained Jurkat cells (lower chamber) from the EC monolayer (upper chamber) via a transwell, the ECs remained negative for PKH67 (Fig. 15D). The last experiment included preincubation (2 h) of the stained Jurkat cells in order to let them shed of vesicles or just lose single dye molecules. When preconditioned supernatant of PKH67 stained Jurkat cells was added onto the endothelial monolayer and EC incubation for 4 h was performed, only 5% of ECs were PKH67$^+$ (Fig. 15E). These results indicated that close cell-cell contact was important for the exchange of membrane patches between Jurkat and endothelial cells which was not mediated by released particles such as exosomes.

The experiment was repeated and the combined data (mean and standard deviation) are shown in Fig. 16.
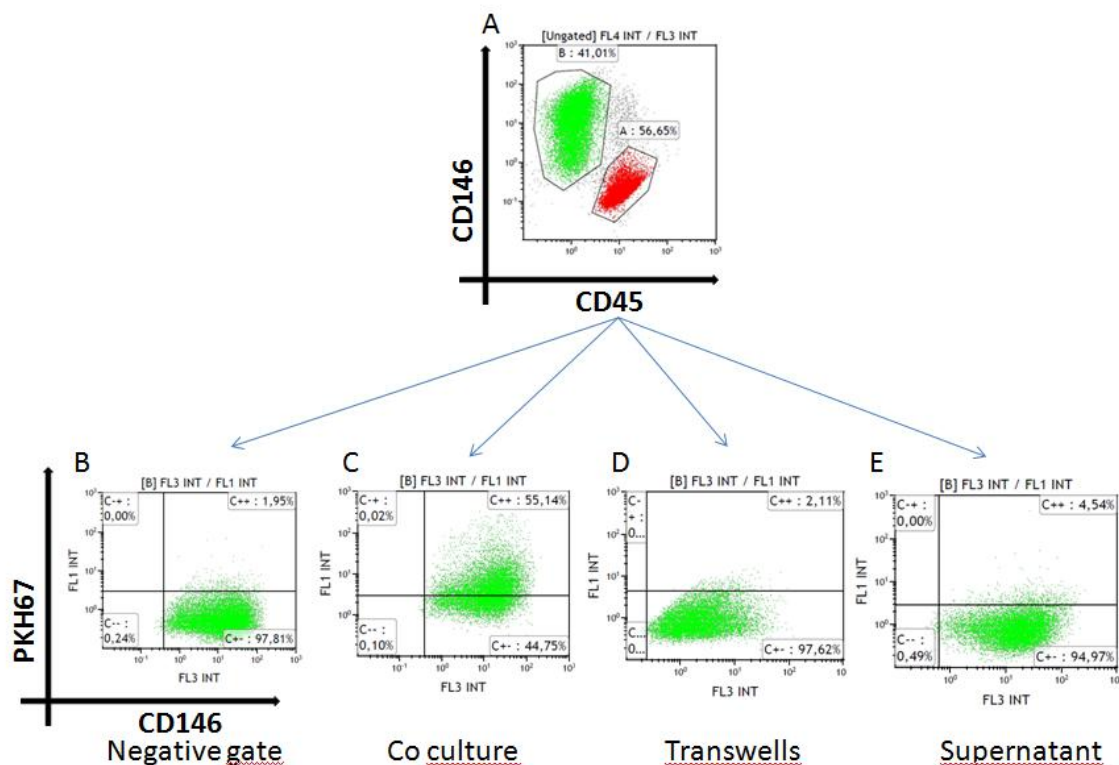
Fig. 15: Intercellular membrane exchange illustrated by PKH67 fluorescence in flow cytometry:

After labeling parental Jurkat cells with 2 µM of the PKH67 membrane dye, a co-culture experiment with ECs was performed for 4 h at an acceptor to donor ratio of 1:5. Cells were harvested and immunostained to distinguish between (A) ECs (CD146) and Jurkat cells (CD45) in flow cytometry. (B) The negative gate was set to 98% of ECs after co-culture with unstained parental Jurkat cells. ECs positive for PKH67 transfer were detected (C) after direct co-culture with PKH67 labeled Jurkat cells or (D) when stained Jurkat cells (lower compartment) were separated from ECs (upper compartment) in a transwell. (E) Conditioned medium of labeled Jurkat cells was added onto the endothelial monolayer for 4 h prior to analysis.
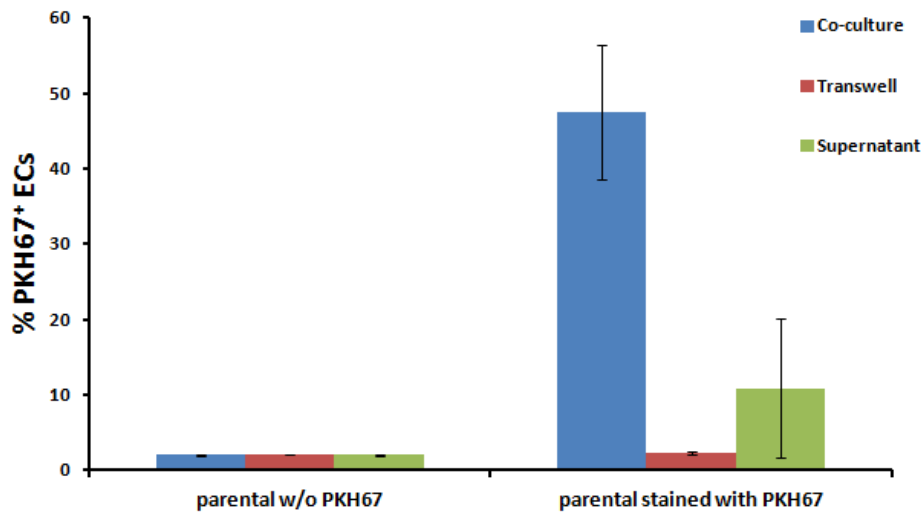
Fig. 16: Membrane transfer from Jurkat cells to ECs detected by PKH67 stain:

Parental Jurkat cells were labeled with 2 μM PKH67 and three different settings were used to monitor membrane transfer to ECs: Labeled Jurkat cells and ECs were co-cultured for 4 h in direct cell contact or were separated via a transwell. Alternatively, labeled Jurkat cells were pre-incubated and only the conditioned supernatant was added onto the endothelial monolayer for 4 h. ECs were harvested, stained and analyzed by flow cytometry for PKH67 fluorescence indicating membrane transfer. Mean values and standard deviation of 2 independent experiments are shown. For negative control, the experiments were conducted with unlabeled Jurkat cells.

3.7 Co-transfer of EGFP-Ras and PKH67 as potential evidence for trogocytosis

To address the question whether trogocytosis was the mechanism of EGFP-Ras transfer from Jurkat cells to ECs, we analyzed whether EGFP-Ras and PKH67-labeled membrane patches were transferred concomitantly from donor cells to acceptor cells. Therefore, Jurkat cells or clones were stained with PKH67 before a co-culture experiment with ECs was performed for 4 hours. Unlabeled Jurkat cells served as negative control.

In comparison to the negative control (Fig. 17A) almost 90% of ECs presented positive for PKH67-labeled membrane exchange after 4 hours of co-culture (Fig. 17B). When Jurkat clones expressing EGFP-Ras variants (C3, ctH, H12V and K12V) were labeled with the lipophilic dye and then used for co-culture, both, the signal of EGFP and of PKH67 increased in the recipient ECs (Fig. 17C-F). While PKH67 transfer was extensive, the number of EGFP+ ECs was comparably moderate: 3% (C3), 16% (ctH), 5% (H12V) and 2% (K12V) of EGFP+

ECs. For all four clones, the cells with the highest uptake of PKH67 were the cells that were also positive for EGFP.
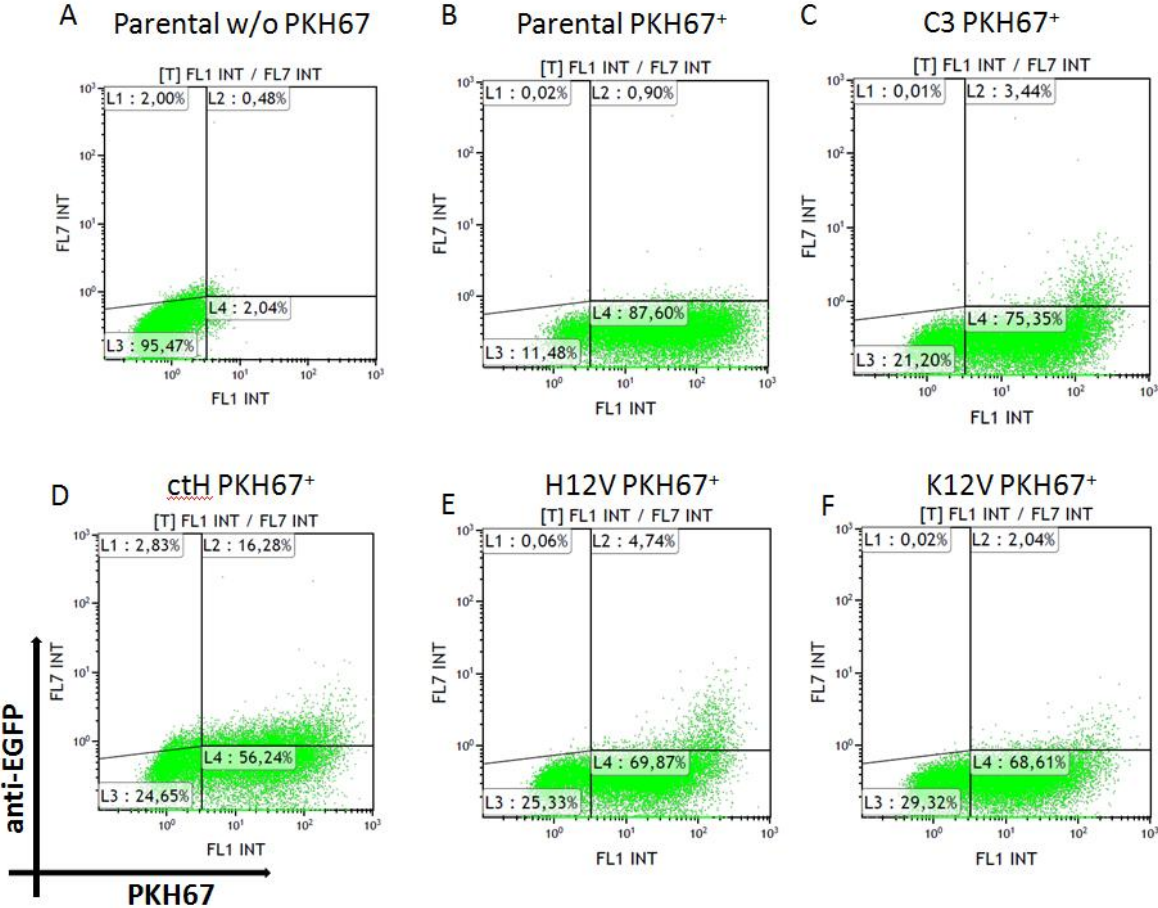
Fig. 17: Co-Transfer of EGFP-Ras variants and PKH67-labeled cell membranes as detected by flow cytometry:

Parental Jurkat cells and Jurkat cell clones (C3, ctH, H12V and K12V) were labeled with 2 µM PKH67 before co-culture with ECs for 4 hours. Unlabeled Jurkat cells served as negative control in co-culture. ECs were harvested, stained and analyzed via flow cytometry for uptake of Jurkat cell membrane (PKH67+) and transfer of EGFP-Ras variants.

3.8 Actin dependence of EGFP-Ras transfer as potential evidence for trogocytosis

To further unravel the transfer mechanism of EGFP-Ras molecules from Jurkat cells onto ECs latrunculin B was tested which is used to inhibit actin polymerization in vitro by disrupting microfilament-mediated processes and which is described to inhibit trogocytosis [77]. With the support of E. Buchberger we incubated ECs with latrunculin B and detected a substantial disturbance of the actin cytoskeleton within 30 min of treatment (Fig. 19 B) compared to untreated ECs (Fig. 19 A).

In our experiment endothelial cells and Jurkat ctH cells were pre-incubated with 1 µM latrunculin B for 30 min followed by a 30 min co-culture. During the co-culture latrunculin B was not present. Cells were subsequently harvested, immunostained for CD146, CD45 and EGFP, and analyzed by flow cytometry. When the co-culture was performed without latrunculin B pretreatment, 36% of ECs were detected positive for EGFP-ctH transfer. The percentage of EGFP$^+$ ECs was diminished by preincubation of ECs with latrunculin B to 33% or by preincubation of Jurkat ctH cells to 26%. If both cell types were exposed to the drug, only 22% of ECs were EGFP$^+$ (Fig. 20). The experiment shows that an active cytoskeleton of the donor as well as the acceptor cell contributes to the intercellular protein transfer between ECs and Jurkat cells but that disruption of the cytoskeleton did not entirely block EGFP-Ras transfer.
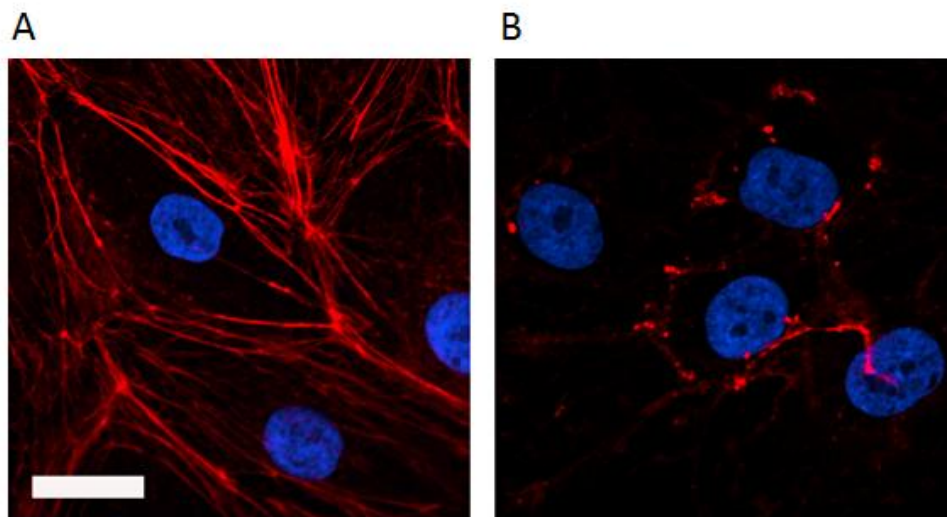
Fig 18: Disruption of the actin cytoskeleton using latrunculin B

Endothelial cells were left untreated (A) or treated with 1 µM latrunculin B for 30 min. ECs were fixed with PFA, permeabilized with TritonX and stained with Phalloidin Alexa Fluor® 647 and Hoechst 33342. Sclace bar: 20 µm.
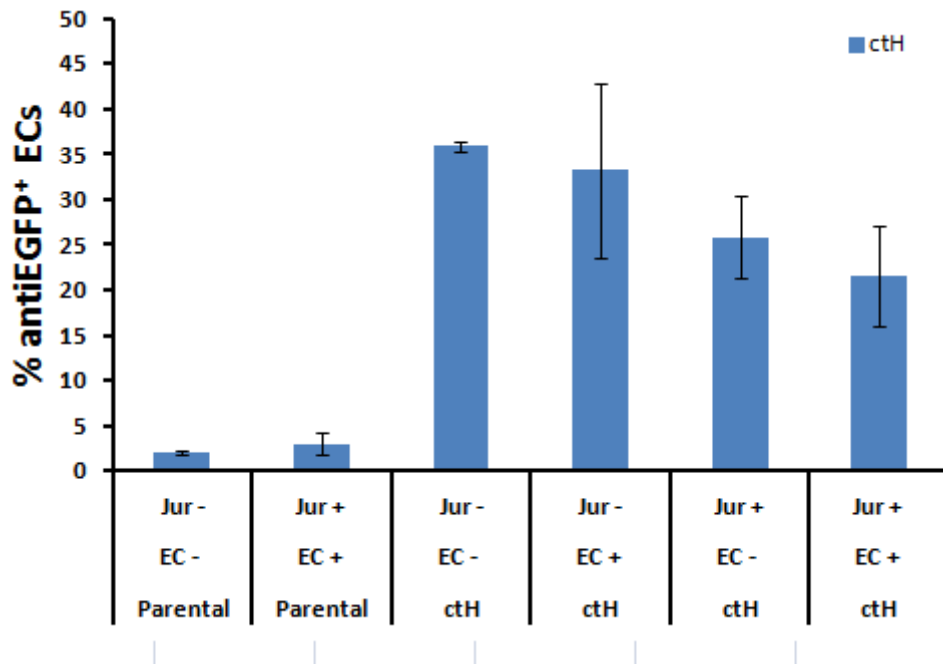
Fig. 20: Reduction of EGFP-Ras transfer by disruption of the actin cytoskeleton:

Co-culture for 30 min of ECs and Jurkat ctH cells untreated (-) or pretreated (+) with 1 μM latrunculin B for 30 min. Cells were harvested, stained and analyzed via flow cytometry for EGFP-ctH transfer. Mean values and standard deviation from 2 independent experiments are shown.

3.9 Functionality of EGFP-Ras upon transfer

In addition to the mechanism of transfer, we addressed the question if the transferred EGFP-Ras molecule is functional in the recipient ECs. The Ras molecule, a small GTPase, is capable of inducing different types of cell responses such as differentiation, proliferation and survival by triggering the respective signaling pathways. Therefore, we investigated if EGFP-Ras can induce the prominent Ras-Raf-MEK-ERK cascade upon transfer from Jurkat cells onto endothelial acceptor cells.

One hour before performing the co-culture the medium of the ECs was changed to EBM-2 + 0.1% BSA which does not contain any growth factors or FCS and should therefore minimize basal ERK activation in ECs. After a 2 h co-culture of ECs and PKH67 stained Jurkat clones (ctH, H12V and K12V) at a ratio of 1:5, the cells were harvested under sterile conditions and prepared for FACsorting by staining for CD146 and CD45.

In previous experiments, the efficient detection of EGFP-Ras transfer to ECs required cell fixation and permeabilization for anti-EGFP antibody staining. However, this approach was not suited for pERK detection, because permeabilization interfered with subsequent pERK detection. Thus, ECs were FACsorted based on their concomitant PKH67 uptake, as cells positive for EGFP-Ras transfer were found to show the highest PKH67 signal (Fig. 17).

The upper 20% PKH67$^+$ ECs were sorted and whole cell lysates were prepared for Western Blot analysis. 2 µg of protein extract were loaded for SDS-PAGE. In Western blotting antibodies against ERK and pERK were used to detect the proteins and analyze the status of ERK activation. The immunoblot showed a strong ERK signal at 42 (ERK-2) and 44 (ERK-1) kDa and a weaker pERK signal at 42 (ERK-2) and 44 (ERK-1) kDa for all three samples. An unknown possibly unspecific band at 75 kDa was also detected (Fig. 21). Of importance, there was no difference in ERK or p-ERK signals between EC extracts after co-culture with Jurkat ctH as compared to Jurkat H12V or K12V cells. Thus, transfer of a constitutively active, full-length EGFP-Ras molecule did not elicit a p-ERK signal beyond the activation state in the control (EGFP-ctH) recipient cells where EGFP was fused to the Ras membrane anchor without signaling capacity.
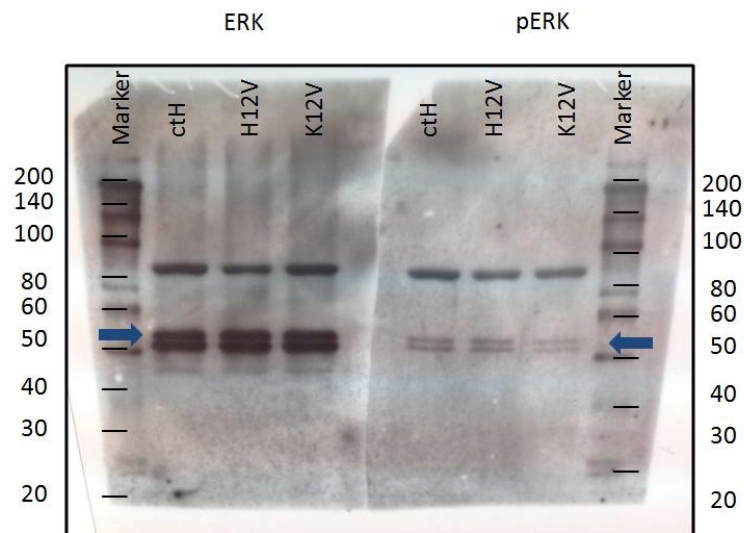
Fig. 19: ERK and pERK levels in ECs after EGFP-Ras transfer:

Jurkat cell clones (ctH, H12V and K12V) were labeled with PKH67 and a co-culture experiment was performed with ECs for 2 h. ECs with a high level of PKH67 transfer (upper 20% of PKH67$^+$ ECs) were FACsorted, cell lysates were prepared and a Western Blot was performed. Membranes were stained with primary rabbit anti-human ERK1/2 (1:1000) and rabbit anti-human phospho-ERK1/2 (1:1000) antibodies followed by secondary goat α-rabbit IgG-HRP-conjugate (1:100.000). Blue arrows indicate the ERK/pERK band at 42 and 44 kDa.

4. DISCUSSION

The transfer of EGFP-Ras molecules from tumor cells (Jurkat cells) onto endothelial cells could previously be demonstrated by Katrin Gitschtaler who conducted the initial experiments leading to this master thesis [74]. In this study further steps were made to elucidate the transfer mechanism in more detail and the following questions were addressed: After successfully verifying the transfer of EGFP-Ras from Jurkat cells onto the recipient ECs in a transendothelial migration assay, the donor to acceptor cell ratio was tested. This was not only performed to optimize EGFP-Ras exchange but to elucidate if the transfer also occurs at low ratios of 1:1 which would represent a more physiological setting. Further aspects such as the time course of protein exchange, the half-life of the transferred EGFP-Ras molecules, and their cellular localization were also investigated. Speed of transfer and retention time of the exchanged molecules were examined using flow cytometry. To gain deeper insight into the cellular localization of the transferred EGFP-Ras molecules, flow cytometry as well as confocal laser scanning microscopy were applied. To elucidate the mechanism of transfer a lipophilic membrane dye that visualizes trogocytosis as well as the actin filament disrupter latrunculin B were applied. Finally, an attempt was made to detect functionality of the transferred Ras molecule in the acceptor cell by immunoblots for ERK phosphorylation.

To conduct the experiments Jurkat clones stably transfected with EGFP-Ras expression constructs were used as donor cells. These clones had previously been generated and kindly provided by Katrin Gitschtaler [74]. The T-cell lymphoma Jurkat cell line was chosen to generate the donor clones because these cells do not carry any endogenous Ras gene mutation [75]. An experimental model of trans-endothelial migration was set up to mimic the process of extravasation where tumor cells and ECs get in very close contact as the tumor cells leave the blood vessel and transmigrate through the endothelium to infiltrate into the tissue. While this metastatic process is commonly associated with solid carcinomas, it also occurs with blood cell derived tumors, e.g. within the bone marrow or organs such as the lung [78]. The notion that tumor cells can transfer Ras molecules, in particular the mutated and constitutively active Ras proteins, to interacting ECs is of interest, since these transferred Ras proteins may be functional in the recipient cell and alter endothelial behavior. For example, Ras signaling is known to trigger a pro-angiogenic EC phenotype characterized by enhanced proliferation and migration which would in turn support tumor cell growth and spread [79-80].

The stably transfected Jurkat clones were expressing different EGFP-Ras fusion molecules: Constructs containing H-RasG12V and K-RasG12V fused to EGFP led to the expression of membrane located and constitutively active Ras molecules. The EGFP-ctH construct expressing a membrane located EGFP due to fusion to the membrane anchor of the Ras molecule, was used as positive control for intercellular protein transfer and as negative control concerning functionality [42]. Furthermore, the pEGFP-C3 control plasmid encoding EGFP without Ras fusion resulted in cytoplasmatic EGFP expression and little protein transfer.

When Katrin Gitschtaler first tested whether EGFP-Ras fusion molecules were transferred from the donor (Jurkat) to the acceptor cell (EC), the transfer was hardly detectable [74]. In contrast, transfer rates as high as 40% were frequently achieved in this master study which was due to a change in detection method. Endothelial cells have a high autofluorescence in the EGFP channel (525 nm emission) in flow cytometric analysis. This fact caused the problem that it was hard to detect the transferred EGFP-Ras molecules in ECs and therefore we introduced the strategy to stain the cells intracellulary with rabbit anti-EGFP and goat anti-rabbit Alexa Fluor® 700 antibodies. This led to the result that two to three times more ECs were detected positive for EGFP after a co-culture experiment with different Jurkat cell clones. We used this strategy for all experiments that followed during this study because the detection via the anti-EGFP signal was more sensitive than using the EGFP signal.

The first question we addressed was the donor to acceptor cell ratio required to promote detectable protein exchange. In our experiments (transendothelial migration assay or co-culture experiments) we evaluated the transfer of the EGFP-Ras fusion molecules from Jurkat cells onto ECs at different ratios (1:1, 1:5 and 1:10). In comparison Rechavi et al. used a ratio of 1:2 in co-culture experiments of various B721-cell transfectants to natural killer cells (NKs) or T cells in order to examine the intercellular transfer of EGFP-tagged molecules [65]. The 1:1 ratio was of particular interest in terms of physiological relevance of the intercellular exchange of Ras molecules between a cancer donor cell passing the endothelial cell layer during extravasation. Katrin Gitschtaler previously tested comparable ratios of 1:3.5, 1:5 and 1:10 and reported the following: the more tumor cells were added onto the EC monolayer, the more tumor cells attached to it, but she did not investigate whether there was a concomitant increase in EGFP-Ras transfer [74]. Using the three distinct donor to acceptor cell ratios we obtained the following results: Even at the lowest ratio of 1:1 protein transfer from Jurkat cells was detectable in 4-10% of ECs, depending on the EGFP-Ras fusion variant. When the cell ratio was increased to 1:5 the amount of EGFP$^+$ ECs increased by about 2-fold. The

difference in protein transfer between a ratio of 1:5 and 1:10 was not as striking as between 1:1 and 1:5 indicating that a plateau was reached at a ratio of 1:5. This might be explained by the observation that at higher ratios (1:10) many Jurkat cells remain in suspension and do not get in close contact with the endothelial monolayer.

In co-culture experiments at 1:5 ratio, the highest transfer rate was generally observed for the Jurkat ctH clone which reached 30-40% of EGFP$^+$ ECs. For Ras H12V and K12V fusion constructs, the transfer rates ranged at 15% and 7%, respectively. This discrepancy in transfer efficiency might relate to protein size or protein expression levels. The ctH construct is the smallest one, because it only consists of the membrane anchor of the Ras molecule fused to EGFP. This might explain why it is more readily transferred during exchange of membrane patches. However, the higher number of EGFP$^+$ ECs for this construct can also come from the fact, that Jurkat cells express this construct at a higher level than the other variants (H12V and K12V). This can be seen comparing the mean fluorescent intensities (MFI values) in flow cytometry. Parental Jurkat cells show autofluorescence equivalent to an MFI of 0.6 in the EGFP detection channel at 525 nm. The Jurkat ctH clone has a fluorescence value around 40 and the other two clones expressing H12V and K12V show an MFI of 10 and 6, respectively. Thus, the expression rate of the fusion molecules is clearly different between the generated clones and this might in turn lead to different transfer rates. Different transfer rates comparing the three different Jurkat clones could also arise because different Ras isoforms have distinct plasma membrane localization. Even though both, H-Ras and K-Ras are highly mobile within the plasma membrane, it has been reported that K-Ras is predominantly located in non-raft plasma membrane structures [81-83]. In contrast, H-Ras is distributed in raft as well as non-raft plasma membrane regions. The distribution of H-Ras between raft and non-raft domains depends on the activation state: activated, GTP bound H-Ras is translocates from raft to non-raft membrane compartments [84]. Therefore, oncogenic H-Ras carrying a mutation in position 12 from glycine to valine that leads to a constitutively active molecule is almost exclusively located in non-raft domains. This means for our experimental situation that the ctH construct (H-Ras membrane anchor fused to EGFP) which is not functional due to the absence of the signaling part of the H-Ras molecule is located in lipid rafts. EGFP-H12V and EGFP-K12V which are constitutively active are expected to be located in non-raft plasma membrane domains. Since we assume that the transfer of the EGFP-Ras molecules is based on trogocytosis the factor of raft domains may play an important role in the context of the exchange of whole membrane patches and its associated molecules. Lipid rafts not only mediate many cellular processes, organize signaling molecules and regulate membrane

trafficking but also have a big influence on membrane fluidity [82]. As it is not the whole membrane that is exchanged but only parts thereof, it is reasonable to assume that there are membrane domains more suited for transfer than others e.g. because of membrane fluidity or protein content.

Having established that membrane-located EGFP-Ras fusion proteins were transferred from Jurkat cells onto interacting ECs, we next evaluated the speed of transfer. The exchange of membrane fragments together with the associated proteins, also known as trogocytosis, is described as being cell-cell contact dependent and very rapid, because it does not require de novo protein synthesis. Hudrisier et al. reported that the transfer of PKH67, a lipophilic membrane dye, from from antigen presenting cells to cytotoxic T-cells could already be detected after 5 min and reached its maximum after 30 min of co-culture [69]. In our experiments we selected the following time points: 15 min, 30 min, 1 h, 2 h and 4 h for the duration of the co-culture of Jurkat cell clones and ECs. For all three clones (ctH, H12V and K12V) we observed a substantial transfer after 15 min. The longer the co-culture continued the higher was the percentage of EGFP$^+$ ECs. However, after a co-culture period of 1-2 h the maximal transfer capacity was reached. This might be explained by the fact that it takes some time until Jurkat cells (in suspension) settle onto the endothelial monolayer and form close cell-cell contact. Hudrisier et al. also claimed that trogocytosis was dependent on surface receptors (e.g. TCR, CD3 and CD28 of T-cells) engaged between the interacting cells [66]. To date, no surface receptors have been described that are required for trogocytosis by endothelial cells. However, numerous adhesion molecules and surface receptors such as selectins or integrins have been identified on ECs which mediate T-cell interaction and attachment and which might also be able to promote membrane exchange [85].

After investigating the speed of protein exchange, the question arose where the transferred EGFP-Ras molecule was located in the recipient endothelial cell: Was it inside the cell i.e. possibly retaining its inner membrane orientation or did it stick to the EC surface? Rechavi et al. verified the intracellular localization of the Ras molecule upon transfer from a human B cell line (B721) to natural killer or T-cells using indirect immunofluorescence staining with anti-Ras antibodies and flow cytometric analysis [65]. Furthermore, using confocal and epifluorescence microscopy they showed that the transferred EGFP H-RasG12V molecule was integrated in the plasma membrane of the recipient NK cell. Using comparable techniques we obtained similar results in our experimental setting of Jurkat cell clones and ECs. We applied the same strategy of cell permeabilization before cell analysis via flow

cytometry. Only upon cell permeabilization the anti-EGFP antibody was able to bind to the transferred EGFP-Ras molecule in ECs while there was little or no EGFP-Ras detection on the surface of non-permeabilized ECs. When we analyzed ECs with confocal laser scanning microscopy we found the transferred EGFP-Ras molecules to be arranged as punctae (dots) in the plasma membrane. This punctate membrane distribution has previously been described in the literature for proteins transferred by trogocytosis [81]. Combining the results of the cell permeabilization and the imaging studies, we can infer that the transferred EGFP-Ras molecules are most likely located in the inner plasma membrane. However, to answer this question conclusively, cryo-electron microscopy combined with antibodies carrying solid gold particles could further be used. This would lead to a higher resolution and would allow to determine in which leaflet of the plasma membrane the molecules are located.

By receiving signaling molecules such as Ras via trogocytosis the signaling capacity of a cell could be altered. This would represent a rapid route of cell activation, if the molecule is already activated (Ras-GTP) and the cell does not need to synthesize a new molecule in order to trigger or strengthen a signaling cascade. In this context, we aimed to monitor the retention of the transferred EGFP-Ras fusion constructs in ECs. Ulsh et al. reported that the half-life of oncogenic H-RasG12V was 20 h [83]. In our experiments we observed a similar half-life of approximately 24 h for transferred EGFP-ctH over a time period of 0 h to 72 h. It should be emphasized though that the ctH construct only contains the membrane anchor of the H-Ras molecule and so its turn-over may not be completely comparable. The two fusion clones of Ras H12V and K12V had a lower transfer rate which made it more difficult to follow the signal over 72 h. In both cases, the EGFP or anti-EGFP signal had almost vanished after 24 h thus indicating that transferred EGFP-Ras molecules would only exert (potential) effects within the first day after transfer. Furthermore, it has to be considered that in our experimental setting the Ras protein was fused to an EGFP sequence. The linkage to such a large molecule could influence the degradation of a protein. To calculate the exact half-lives of these fusion proteins, additional pulse-chase experiments could be performed as has been done by Ulsh et al [83].

In recent years we have learned that cells can exceed their limitations given by the transcriptome via intercellular protein transfer. This transfer is conducted by the following mechanisms: exocytosis, microvesicles, tunneling nanotubes or trogocytosis [86]. Since previous work on the exchange of Ras molecules between B- and T-cells had identified trogocytosis as the mode of transfer [65], we applied several methods to comparably test for

trogocytosis in our setting. In our experiments we introduced a lipophilic membrane dye called PKH67 which allowed us to monitor the exchange of cell membrane. To address the question whether trogocytosis occurred between Jurkat cells and ECs, we designed three different experimental conditions: We labeled the parental Jurkat cells with the dye and performed a normal co-culture experiment with ECs. A comparable experiment was performed where the cells were separated by a transwell thereby avoiding direct cell-cell contact. In the last setting, labeled Jurkat cells were preincubated and only the supernatant, containing possible microvesicles or released dye molecules, was transferred onto a confluent EC monolayer. In the co-culture setting about 50% of ECs were detected positive for PKH67 after 4 h. This result indicates that membrane patches incorporating the dye are transferred from the labeled Jurkat cells onto the recipient ECs if close cell-cell contact is given. Not only T cells but also B cells or dendritic cells can shed exosomes or microvesicles containing proteins and microRNAs capable of modulating the expression profile of the recipient cell [87]. These vesicles are released by the donor and may promote the transfer without direct cell interactions. When the labeled parental Jurkat cells were separated from the ECs via a transwell no transfer of the dye was observed. When the supernatant of labeled Jurkat cells was transferred onto the ECs, only ~10% of ECs became PKH67$^+$. Thus, the transfer efficiency of the dye was highly reduced when no close cell-cell contact was given indicating that trogocytosis was the preferred route of membrane exchange between Jurkat cells and ECs. The small percentage of PKH67$^+$ ECs in the presence of Jurkat-conditioned supernatant could be explained by an additional (minor) exchange route involving exosomes or microparticles. The fact that no PKH67 transfer was observed in the transwell setting may relate to the possibility that exosomes or microvesicles unspecifically bind to the transwell (plastic) and are not readily passed on to the upper compartment with endothelial cells.

In the next step we checked if the introduced dye and the EGFP-Ras fusion constructs were transferred simultaneously from Jurkat cells to ECs. Therefore, Jurkat cells or clones were labeled with the dye before a co-culture experiment with endothelial cells was performed. Using labeled parental Jurkat cells no double positive ECs were detected. Only when the Jurkat cell clones were prelabeled with membrane dye, the ECs were detected PKH67$^+$ and EGFP$^+$ in flow cytometric analysis. Again, the highest transfer of EGFP-Ras was observed for the ctH clone, followed by H12V and K12V. In contrast, the transfer of the PKH67 dye was comparable between clones. While the majority (70-90%) of ECs had adopted the membrane dye, only a fraction thereof (up to 15%) presented also positive for EGFP-Ras transfer. This divergence in transfer rates may be due to staining intensity or detection sensitivity for the

two molecules. Membrane labeling of Jurkat cells with PKH67 resulted in a high fluorescence intensity (MFI of 20) which exceeded the MFI values for the EGFP fusion constructs (MFI of parental, C3, ctH, H12V and K12V when detected via anti-EGFP antibody: 0, 5, 14, 7, 2). Thus, PKH67 transfer to ECs may more readily be detected and represent membrane exchange rates between cells while transfer of EGFP-Ras molecules by anti-EGFP antibody is less sensitive and only detected for a fraction of cells with extensive transfer, especially in the case of the Jurkat ctH clone (MFI of 14). This notion was supported by the observation that only ECs highly positive for PKH67 were also positive for EGFP and further led to the strategy of FACsorting PKH67^{high} ECs (20%) to isolate and enrich cells with transferred EGFP-Ras molecules.

Apart from the use of membrane dyes, other methods are commonly applied to elucidate whether protein exchange is based on trogocytosis. Several groups have reported that the actin cytoskeleton plays a central role in this process and that trogocytosis is blocked upon disruption of actin filaments [63, 71]. In our experiment we used latrunculin B to inhibit actin polymerization in order to block trogocytosis. To perform the experiment we chose the Jurkat ctH clone because it showed the highest transfer efficiency compared to the other H12V and K12V constructs. When only the donor or acceptor cell was incubated with the drug, the transfer was moderately lowered compared to untreated cells. If both cell types were incubated with latrunculin B for 30 min prior to co-culture EGFP-ctH transfer was reduced by 40%. These results show that disrupting the actin cytoskeleton lowers the transfer efficiency and are in line with other groups that could block trogocytosis of e.g. T-cells with latrunculin B [70]. When the drug was added onto the confluent EC monolayer and incubated for 30 min the cells were visibly changed in their morphology. This limited the duration of the experiment because the endothelial cells lost their ability to form a monolayer and adhere to the bottom with prolonged exposure to latrunculin B. As both cell types, Jurkat cells and ECs, were incubated with latrunculin B, their ability to adhere to each other was also reduced and this may be an additional reason why the transfer efficiency was lowered. To avoid this problem, cells could be brought in close contact by centrifugation as has been done by Ralston et al [88].

In light of the physiological phenomenon of tumor cell extravasation through the endothelial monolayer it seems conceivable that the exchange of whole membrane fragments and associated proteins is a quick process to transfer activated signaling molecules (e.g. oncogenic Ras-GTP) from the donor tumor cell to the acceptor endothelial cell and trigger or strengthen

a respective signal in the recipient cell. Thus, the last experiment of this master thesis was designed to test for enhanced Ras signaling (resulting in the prominent Ras-Raf-MEK-ERK activation pathway) in the recipient ECs.

FACsorting of PKH67^{high} ECs was conducted after a 2 h of co-culture with Jurkat clones to enrich for cells with extensive membrane exchange. EC cell extracts were prepared and an immunoblot was performed. Both, the total levels of ERK1/2 as well as the phosphorylated ERK1/2 proteins were readily detected in EC extracts. However, the Western Blot did not show any difference between the transfer of the non functional EGFP-ctH construct or the constitutively active constructs of EGFP-Ras H12V or K12V. Since the transfer of H12V and K12V was generally low, the amount of constitutively active protein may not have been high enough to further enhance the level of ERK phosphorylation in ECs that is triggered by the mere surface contact between Jurkat cells and ECs in cell culture. A further limitation is the applied sorting strategy. Sorting of the PKH67^{high} ECs is an indirect way of enriching for EGFP-Ras[+] ECs. Provided that cell fixation and permeabilization does not interfere with pERK detection by Western blot, the staining and sorting strategy based on anti-EGFP antibody could be used in a further attempt to detect enhanced Ras signaling upon EGFP-Ras H12V or K12V transfer.

In summary, the experimental work of this master thesis revealed that Ras protein transfer from Jurkat cells to ECs differed depending on the EGFP-Ras fusion construct. Investigations regarding the subcellular localization, the speed of transfer and the half-life of the transferred molecules led to the following results: The exchange occurs rapidly and transferred molecules are located intracellulary and incorporated in the plasma membrane. The half-life of the transferred EGFP-Ras fusion proteins is about 24 h. Furthermore, we can say that close cell-cell contact is indispensible for the intercellular membrane and protein transfer. Trogocytosis may not be the only mechanism of exchange between Jurkat cells and ECs, since a moderate transfer was achieved by the soluble fraction (supernatant) and EGFP-Ras transfer was not entirely blocked upon disruption of the actin cytoskeleton. In this study no functional consequence of EGFP-Ras transfer from Jurkat cells to ECs could be proven, but functional experiments were limited and assay optimization may be required.

In future work, more emphasis has to be given to testing the (potential) functional consequences of oncogenic EGFP-Ras transfer to ECs such as enhanced proliferation and

migration. Furthermore, the in vitro findings shall be extended to an in vivo mouse model by injecting Jurkat clones into immunocompromised mice to possibly gain in vivo evidence for the occurrence of oncogenic Ras transfer from tumor to endothelial cells.

5. REFERENCES

1. Chang, E.H., et al., *Human genome contains four genes homologous to transforming genes of Harvey and Kirsten murine sarcoma viruses.* Proc Natl Acad Sci U S A, 1982. 79(6289320): p. 4848-4852.

2. Malumbres, M. and M. Barbacid, *RAS oncogenes: the first 30 years.* Nat Rev Cancer, 2003. 3(6): p. 459-65.

3. Shimizu, K., et al., *Isolation and preliminary characterization of the transforming gene of a human neuroblastoma cell line.* Proc Natl Acad Sci U S A, 1983. 80(2): p. 383-7.

4. Mitin, N., K.L. Rossman, and C.J. Der, *Signaling interplay in Ras superfamily function.* Curr Biol, 2005. 15(16051167): p. 563-574.

5. Omerovic, J., A.J. Laude, and I.A. Prior, *Ras proteins: paradigms for compartmentalised and isoform-specific signalling.* Cell Mol Life Sci, 2007. 64(19-20): p. 2575-89.

6. Wennerberg, K., K.L. Rossman, and C.J. Der, *The Ras superfamily at a glance.* J Cell Sci, 2005. 118(15731001): p. 843-846.

7. Henis, Y.I., J.F. Hancock, and I.A. Prior, *Ras acylation, compartmentalization and signaling nanoclusters (Review).* Mol Membr Biol, 2009. 26(1): p. 80-92.

8. Hancock, J.F., et al., *A CAAX or a CAAL motif and a second signal are sufficient for plasma membrane targeting of ras proteins.* EMBO J, 1991. 10(1756714): p. 4033-4039.

9. Otto, J.C., et al., *Cloning and characterization of a mammalian prenyl protein-specific protease.* J Biol Chem, 1999. 274(13): p. 8379-82.

10. Desrosiers, R.R., Q.T. Nguyen, and R. Beliveau, *The carboxyl methyltransferase modifying G proteins is a metalloenzyme.* Biochem Biophys Res Commun, 1999. 261(3): p. 790-7.

11. Chen, Y.X., et al., *Synthesis of the Rheb and K-Ras4B GTPases.* Angew Chem Int Ed Engl, 2010. 49(35): p. 6090-5.

12. Apolloni, A., et al., *H-ras but not K-ras traffics to the plasma membrane through the exocytic pathway.* Mol Cell Biol, 2000. 20(7): p. 2475-87.

13. Choy, E., et al., *Endomembrane trafficking of ras: the CAAX motif targets proteins to the ER and Golgi.* Cell, 1999. 98(1): p. 69-80.

14. Wang, G. and R.J. Deschenes, *Plasma membrane localization of Ras requires class C Vps proteins and functional mitochondria in Saccharomyces cerevisiae.* Mol Cell Biol, 2006. 26(16581797): p. 3243-3255.

15. Ashery, U., et al., *Nonconventional trafficking of Ras associated with Ras signal organization.* Traffic, 2006. 7(9): p. 119-26.

16. Campbell, S.L., et al., *Increasing complexity of Ras signaling.* Oncogene, 1998. 17(11 Reviews): p. 1395-413.

17. Huang, H., et al., *Defining the specificity space of the human SRC homology 2 domain.* Mol Cell Proteomics, 2008. 7(17956856): p. 768-784.

18. Hilger, R.A., M.E. Scheulen, and D. Strumberg, *The Ras-Raf-MEK-ERK pathway in the treatment of cancer.* Onkologie, 2002. 25(6): p. 511-8.

19. Rao, V.N. and E.S. Reddy, *elk-1 proteins interact with MAP kinases.* Oncogene, 1994. 9(7): p. 1855-60.

20. Pruitt, K. and C.J. Der, *Ras and Rho regulation of the cell cycle and oncogenesis.* Cancer Lett, 2001. 171(11485822): p. 1-10.

21. Rodriguez-Viciana, P., et al., *Phosphatidylinositol-3-OH kinase as a direct target of Ras.* Nature, 1994. 370(6490): p. 527-32.

22. Bader, A.G., et al., *Oncogenic PI3K deregulates transcription and translation.* Nat Rev Cancer, 2005. 5(12): p. 921-9.

23. Brunet, A., et al., *Akt promotes cell survival by phosphorylating and inhibiting a Forkhead transcription factor.* Cell, 1999. 96(6): p. 857-68.

24. Hennessy, B.T., et al., *Exploiting the PI3K/AKT pathway for cancer drug discovery.* Nat Rev Drug Discov, 2005. 4(12): p. 988-1004.

25. Schubbert, S., K. Shannon, and G. Bollag, *Hyperactive Ras in developmental disorders and cancer.* Nat Rev Cancer, 2007. 7(4): p. 295-308.

26. Filomena, A., A. Paolo, and R. Emilia, *Gastric Cancer: Molecular Pathology State*. 2013.

27. Donovan, S., K.M. Shannon, and G. Bollag, *GTPase activating proteins: critical regulators of intracellular signaling.* Biochim Biophys Acta, 2002. 1602(1): p. 23-45.

28. Bruce Alberts, D.B., Julian Lewis, *Molecular biology of the cell 4th edition.* 2002.

29. Bos, J.L., *ras oncogenes in human cancer: a review.* Cancer Res, 1989. 49(17): p. 4682-9.

30. Downward, J., *Targeting RAS signalling pathways in cancer therapy.* Nat Rev Cancer, 2003. 3(1): p. 11-22.

31. Grewal, T., et al., *Differential Regulation of RasGAPs in Cancer.* Genes Cancer, 2011. 2(3): p. 288-97.

32. Buhrman, G., et al., *Allosteric modulation of Ras positions Q61 for a direct role in catalysis.* Proc Natl Acad Sci U S A, 2010. 107(11): p. 4931-6.

33. Lobell, R.B., et al., *Evaluation of farnesyl:protein transferase and geranylgeranyl:protein transferase inhibitor combinations in preclinical models.* Cancer Res, 2001. 61(24): p. 8758-68.

34. Crooke, S.T., *Potential roles of antisense technology in cancer chemotherapy.* Oncogene, 2000. 19(56): p. 6651-9.

35. Allen, L.F., J. Sebolt-Leopold, and M.B. Meyer, *CI-1040 (PD184352), a targeted signal transduction inhibitor of MEK (MAPKK).* Semin Oncol, 2003. 30(5 Suppl 16): p. 105-16.

36. Dudley, D.T., et al., *A synthetic inhibitor of the mitogen-activated protein kinase cascade.* Proc Natl Acad Sci U S A, 1995. 92(17): p. 7686-9.

37. Favata, M.F., et al., *Identification of a novel inhibitor of mitogen-activated protein kinase kinase.* J Biol Chem, 1998. 273(9660836): p. 18623-18632.

38.   de Bono, J.S. and E.K. Rowinsky, *The ErbB receptor family: a therapeutic target for cancer.* Trends Mol Med, 2002. 8(11927283): p. 19-26.

39.   Fabbro, D., D. Parkinson, and A. Matter, *Protein tyrosine kinase inhibitors: new treatment modalities?* Curr Opin Pharmacol, 2002. 2(4): p. 374-81.

40.   Wakeling, A.E., *Epidermal growth factor receptor tyrosine kinase inhibitors.* Curr Opin Pharmacol, 2002. 2(12127870): p. 382-387.

41.   Bamford, S., et al., *The COSMIC (Catalogue of Somatic Mutations in Cancer) database and website.* Br J Cancer, 2004. 91(2): p. 355-8.

42.   Rechavi, O., I. Goldstein, and Y. Kloog, *Intercellular exchange of proteins: the immune cell habit of sharing.* FEBS Lett, 2009. 583(11): p. 1792-9.

43.   Cocucci, E., G. Racchetti, and J. Meldolesi, *Shedding microvesicles: artefacts no more.* Trends Cell Biol, 2009. 19(19144520): p. 43-51.

44.   Fevrier, B. and G. Raposo, *Exosomes: endosomal-derived vesicles shipping extracellular messages.* Curr Opin Cell Biol, 2004. 16(15261674): p. 415-421.

45.   Simons, M. and G. Raposo, *Exosomes--vesicular carriers for intercellular communication.* Curr Opin Cell Biol, 2009. 21(19442504): p. 575-581.

46.   Faure, J., et al., *Exosomes are released by cultured cortical neurones.* Mol Cell Neurosci, 2006. 31(16446100): p. 642-648.

47.   Smalheiser, N.R., *Exosomal transfer of proteins and RNAs at synapses in the nervous system.* Biol Direct, 2007. 2(18053135): p. 35-35.

48.   Ahmed, K.A. and J. Xiang, *Mechanisms of cellular communication through intercellular protein transfer.* J Cell Mol Med, 2011. 15(7): p. 1458-73.

49.   van der Pol, E., et al., *Classification, functions, and clinical relevance of extracellular vesicles.* Pharmacol Rev, 2012. 64(3): p. 676-705.

50.   van Niel, G., et al., *Exosomes: a common pathway for a specialized function.* J Biochem, 2006. 140(1): p. 13-21.

51.   Hu, G., K.M. Drescher, and X.M. Chen, *Exosomal miRNAs: Biological Properties and Therapeutic Potential.* Front Genet, 2012. 3: p. 56.

52.   Ogata-Kawata, H., et al., *Circulating exosomal microRNAs as biomarkers of colon cancer.* PLoS One, 2014. 9(4): p. e92921.

53.   Raposo, G. and W. Stoorvogel, *Extracellular vesicles: exosomes, microvesicles, and friends.* J Cell Biol, 2013. 200(4): p. 373-83.

54.   Belting, M. and A. Wittrup, *Nanotubes, exosomes, and nucleic acid-binding peptides provide novel mechanisms of intercellular communication in eukaryotic cells: implications in health and disease.* J Cell Biol, 2008. 183(19103810): p. 1187-1191.

55.   Chinnery, H.R., E. Pearlman, and P.G. McMenamin, *Cutting edge: Membrane nanotubes in vivo: a feature of MHC class II+ cells in the mouse cornea.* J Immunol, 2008. 180(9): p. 5779-83.

56. Onfelt, B., et al., *Cutting edge: Membrane nanotubes connect immune cells.* J Immunol, 2004. 173(15265877): p. 1511-1513.

57. Quah, B.J.C., et al., *Bystander B cells rapidly acquire antigen receptors from activated B cells by membrane transfer.* Proc Natl Acad Sci U S A, 2008. 105(18337504): p. 4259-4264.

58. Sherer, N.M., et al., *Retroviruses can establish filopodial bridges for efficient cell-to-cell transmission.* Nat Cell Biol, 2007. 9(17293854): p. 310-315.

59. Sowinski, S., et al., *Membrane nanotubes physically connect T cells over long distances presenting a novel route for HIV-1 transmission.* Nat Cell Biol, 2008. 10(18193035): p. 211-219.

60. Onfelt, B., et al., *Structurally distinct membrane nanotubes between human macrophages support long-distance vesicular traffic or surfing of bacteria.* J Immunol, 2006. 177(12): p. 8476-83.

61. Davis, D.M. and S. Sowinski, *Membrane nanotubes: dynamic long-distance connections between animal cells.* Nat Rev Mol Cell Biol, 2008. 9(6): p. 431-6.

62. Rustom, A., et al., *Nanotubular highways for intercellular organelle transport.* Science, 2004. 303(5660): p. 1007-10.

63. Joly, E. and D. Hudrisier, *What is trogocytosis and what is its purpose?* Nat Immunol, 2003. 4(9): p. 815.

64. Huang, J.F., et al., *TCR-Mediated internalization of peptide-MHC complexes acquired by T cells.* Science, 1999. 286(10542149): p. 952-954.

65. Rechavi, O., et al., *Intercellular transfer of oncogenic H-Ras at the immunological synapse.* PLoS One, 2007. 2(11): p. e1204.

66. Hudrisier, D., et al., *Capture of target cell membrane components via trogocytosis is triggered by a selected set of surface molecules on T or B cells.* J Immunol, 2007. 178(6): p. 3637-47.

67. Mainiero, F., et al., *Integrin-mediated ras-extracellular regulated kinase (ERK) signaling regulates interferon gamma production in human natural killer cells.* J Exp Med, 1998. 188(9763606): p. 1267-1275.

68. Tabiasco, J., et al., *Acquisition of viral receptor by NK cells through immunological synapse.* J Immunol, 2003. 170(12): p. 5993-8.

69. Hudrisier, D., et al., *Cutting edge: CTLs rapidly capture membrane fragments from target cells in a TCR signaling-dependent manner.* J Immunol, 2001. 166(11238601): p. 3645-3649.

70. Aucher, A., et al., *Capture of plasma membrane fragments from target cells by trogocytosis requires signaling in T cells but not in B cells.* Blood, 2008. 111(12): p. 5621-8.

71. Genot, E. and D.A. Cantrell, *Ras regulation and function in lymphocytes.* Curr Opin Immunol, 2000. 12(10781411): p. 289-294.

72. McCann, F.E., et al., *The activating NKG2D ligand MHC class I-related chain A transfers from target cells to NK cells in a manner that allows functional consequences.* J Immunol, 2007. 178(17339436): p. 3418-3426.

73.   Vernitsky, H., et al., *Ras oncoproteins transfer from melanoma cells to T cells and modulate their effector functions.* J Immunol, 2012. 189(9): p. 4361-70.

74.   Gitschtaler, K., *Master-Thesis: Transfer of Oncogenic Ras Protein from Tumor Cells onto Interacting Endothelial Cells*. 2013, University of Vienna.

75.   Perez de Castro, I., et al., *Ras activation in Jurkat T cells following low-grade stimulation of the T-cell receptor is specific to N-Ras and occurs only on the Golgi apparatus.* Mol Cell Biol, 2004. 24(15060167): p. 3485-3496.

76.   Rousselle, C., et al., *Innocuousness and intracellular distribution of PKH67: a fluorescent probe for cell proliferation assessment.* In Vitro Cell Dev Biol Anim, 2001. 37(10): p. 646-55.

77.   Waschbisch, A., et al., *Intercellular exchanges of membrane fragments (trogocytosis) between human muscle cells and immune cells: a potential mechanism for the modulation of muscular immune responses.* J Neuroimmunol, 2009. 209(1-2): p. 131-8.

78.   Ito, M., et al., *MicroRNA-150 inhibits tumor invasion and metastasis by targeting the chemokine receptor CCR6, in advanced cutaneous T-cell lymphoma.* Blood, 2014. 123(10): p. 1499-511.

79.   Meadows, K.N., et al., *Activated Ras induces a proangiogenic phenotype in primary endothelial cells.* Oncogene, 2004. 23(1): p. 192-200.

80.   Serban, D., J. Leng, and D. Cheresh, *H-ras regulates angiogenesis and vascular permeability by activation of distinct downstream effectors.* Circ Res, 2008. 102(11): p. 1350-8.

81.   Pham, T., P. Mero, and J.W. Booth, *Dynamics of macrophage trogocytosis of rituximab-coated B cells.* PLoS One, 2011. 6(1): p. e14498.

82.   Pike, L.J., *The challenge of lipid rafts.* J Lipid Res, 2009. 50 Suppl(18955730): p. 323-328.

83.   Ulsh, L.S. and T.Y. Shih, *Metabolic turnover of human c-rasH p21 protein of EJ bladder carcinoma and its normal cellular and viral homologs.* Mol Cell Biol, 1984. 4(8): p. 1647-52.

84.   Hancock, J.F., *Ras proteins: different signals from different locations.* Nat Rev Mol Cell Biol, 2003. 4(5): p. 373-84.

85.   Hogg, N., et al., *T-cell integrins: more than just sticking points.* J Cell Sci, 2003. 116(Pt 23): p. 4695-705.

86.   Davis, D.M., *Intercellular transfer of cell-surface proteins is common and can affect many stages of an immune response.* Nat Rev Immunol, 2007. 7(3): p. 238-43.

87.   Mittelbrunn, M., et al., *Unidirectional transfer of microRNA-loaded exosomes from T cells to antigen-presenting cells.* Nat Commun, 2011. 2: p. 282.

88.   Ralston, K.S., et al., *Trogocytosis by Entamoeba histolytica contributes to cell killing and tissue invasion.* Nature, 2014. 508(7497): p. 526-30.

6. APPENDIX

6.1 LIST OF ABBREVIATIONS

AA	acrylamide
Akt	protein kinase B (PKB)
APC	antigen presenting cell
APS	ammonium persulfate
BAD	bcl-2-associated death promoter
BCA	bicinchoninic acid
BSA	bovine serum albumin
CFC	cardio-facio-cutaneous
CLSM	confocal laser scanning microscopy
CMV	cytomegalovirus
ctH	C-terminal tail of H-Ras
ddH$_2$O	double distilled water
DMSO	dimethylsulfoxide
DTT	dithiothreitol
EBM	endothelial basal medium
EC	endothelial cell
EGF	epidermal growth factor
EGFP	enhanced green fluorescence protein
EGFR	epidermal growth factor receptor
EGM	endothelial growth medium
ELK1	ETS domain-containing protein
ER	endoplasmic reticulum
ERK	extracellular signal-regulated kinase
f.c.	final concentration
FCS	fetal calf serum
FKHR	forkhead
FTI	farnesyltransfeRase inhibitors
GAP	GTPase activating protein

GDP	guanosine diphosphate
GEF	guanine nucleotide exchange factor
GFs	growth factors
GFP	green fluorescence protein
GRB2	growth factor receptor bound protein 2
GTP	guanosine triphosphate
HEPES	4-(2-hydroxyethyl)-1-piperazineethanesulfonic acid
HRP	horseradish peroxidase
HIV-1	human immunodeficiency virus
HVR	hypervariable region
Icmt	isoprenyl cysteine transfeRase
IFNγ	interferon gamma
IL1β	interleukin 1 beta
iNKT	invariant natural killer T cells
IS	immunological synapse
LEC	lymphatic endothelial cell
MCAM	melanoma cell adhesion molecule
MEK	mitogen-activated protein kinase kinase
MFI	mean fluorescence intensity
MHC	major histocompatibility complex
MLV	murine leukemia virus
MVB	multivesicular bodies
MVE	multivesicular endosomes
NK	natural killer cell
pAg	phosphoantigen
PBMC	peripheral blood mononuclear cell
PBS	phosphate buffered saline
PDK1	3-phosphoinositide-dependent protein kinase 1
PI3K	phosphatidylinositol-3-kinase
PIP$_2$	phosphatidylinositol-4,5-bisphosphate
PIP$_3$	phosphatidylinositol-3,4,5-triphosphate
Raf	rapidly accelerated fibrosarcoma
RalGDS	Ral guanine nucleotide-dissociation stimulator
Rce1	Ras-converting enzyme 1

RT	room temperature
SDS	sodium dodecyl sulfate
SHC1	SHC-transforming protein 1
SOS	Son of Sevenless
Src	Proto-oncogene tyrosine-protein kinase
TCR	T-cell receptor
TEM	Transendothelial migration assay
TEMED	N,N,N′,N′-Tetramethylethane-1,2-diamine
TNFα	tumor necrosis factor alpha
TNTs	Tunneling nano-tubes
TW	transwell
VEGF	vascular endothelial growth factor
w/o	without
β-SH	β-mercaptoethanol

6.2 ABSTRACT

Interacting cells are capable of exchanging entire membrane patches. Thus, functional surface molecules as well as membrane-associated components of the intracellular signaling cascade (e.g. Ras) may transfer from one cell to the other to initiate intracellular signals in the recipient cell. These effects have mainly been reported for leukocyte-leukocyte interactions. Endothelial cells (ECs) form a barrier in the human body between blood/lymph and tissue and play a major role in inflammatory and metastatic processes where leukocytes or tumor cells have to pass the endothelium to invade the tissue. In this context, we aimed to investigate the transfer of membrane-associated Ras signaling molecules from T-lymphoma cells (Jurkat cells) to interacting ECs. This question seemed of particular interest, since mutated, constitutively active Ras proteins are found in the most common types of cancer and active Ras molecules may trigger endothelial cell responses such as proliferation, migration and angiogenesis. To investigate the transfer of oncogenic Ras from tumor to endothelial cells in this master study, trans-migration and co-culture experiments of ECs with transfected Jurkat clones stably expressing EGFP-Ras fusion proteins were conducted. ECs were analyzed by flow cytometry or confocal laser scanning microscopy for EGFP-Ras uptake. An exchange of EGFP-Ras molecules was observed at physiologically relevant, low donor to acceptor cell ratios. The proteins were incorporated into the EC membrane with intracellular orientation. The transfer of EGFP-Ras fusion proteins was rapid, occurred within 15 min and reached a maximum after 1 hour. Once acquired, the EGFP-Ras protein was retained by the recipient ECs with an approximate half-life of 24 hours. The mechanism of transfer was (at least in part) based on trogocytosis which was illustrated by the exchange of entire membrane patches via direct cell-to-cell contact involving the actin cytoskeleton. To conclude the project, one functional experiment was conducted which failed to detect enhanced Ras-Raf-MEK-ERK signaling in recipient ECs upon transfer of mutant EGFP- Ras protein. In summary, transfer of oncogenic Ras from Jurkat lymphoma to endothelial cells was readily observed and characterized at the mechanistic level. Assessment of functional consequences requires further investigation.

6.3 ZUSAMMENFASSUNG

Interagierende Zellen können Membranstücke austauschen. Dieses Phänomen ermöglicht es, dass funktionelle Oberflächenmoleküle sowie Membran-assoziierte Komponenten der intrazellulären Signalkaskaden (wie beispielsweise Ras) von einer Zelle auf eine andere übertragen werden und dort ein Signal auslösen. Diese Effekte wurden bisher vorwiegend für die Interaktion zwischen Leukozyten beobachtet. Endothelzellen bilden eine Schicht im menschlichen Körper, die das Blut oder die Lymphflüssigkeit vom Gewebe trennt. Sie spielen eine wichtige Rolle bei Entzündungsprozessen sowie in der Metastasierung, wo Leukozyten bzw. Tumorzellen durch das Endothel wandern, um ins Gewebe einzudringen. In dieser Master Arbeit wurde der Transfer von Membran-assoziierten Ras Molekülen von Lymphomzellen (Jurkat Zellen) auf interagierende Endothelzellen untersucht. Diese Frage ist von Interesse, da mutierte und dadurch konstitutiv aktive Ras Proteine in den häufigsten Krebsarten zu finden sind und bei Transfer in Endothelzellen Effekte wie Zellteilung, Migration oder Angiogenese auslösen könnten. Um den Transfer von onkogenen Ras Molekülen zu untersuchen, wurden Transmigrationsversuche und Co-Kultur Experimente mit Endothelzellen und stabil transfizierten Jurkat Zellen durchgeführt, die verschiedene EGFP-markierte Ras Proteine exprimierten. Endothelzellen wurden entweder mittels Durchflusszytometrie oder konfokaler Lasermikroskopie untersucht, um die Aufnahme eines EGPF-Ras Moleküls nachzuweisen. Der Austausch von EGFP-Ras Molekülen konnte bereits bei einem physiologisch relevanten, niedrigen Verhältnis von Donor- zu Akzeptor-Zellen nachgewiesen werden. Die übertragenen Proteine zeigten Membranverankerung in den Endothelzellen und waren intrazellulär ausgerichtet. Der Transfer der EGFP-Ras Moleküle war bereits nach 15 Minuten ersichtlich und erreichte nach 1 h ein Maximum. Die übertragenen EGFP-Ras Moleküle hatten eine Halbwertszeit von 24 h. Der Mechanismus des Transfers basierte (zumindest zu einem Großteil) auf Trogozytose, wie durch den Austausch von ganzen Membranstücken unter Zell-Zell Kontakt und Beteiligung des Aktinzytoskeletts gezeigt werden konnte. Zum Abschluss der Master Arbeit wurde ein weiteres Experiment zur Funktionalität des transferierten Ras Moleküls durchgeführt. Dieses Experiment konnte kein verstärktes Ras-Raf-MEK-ERK Signal nach Transfer der konstitutiv aktiven Ras Moleküle in Endothelzellen nachweisen. Zusammenfassend lässt sich feststellen, dass im Rahmen dieser Master Arbeit der Transfer von onkogenen Ras Molekülen von Jurkat Zellen auf Endothelzellen gezeigt und mechanistisch charakterisiert werden konnte. Die Analyse der Funktionalität des übertragenen Moleküls erfordert weitere Untersuchungen.

6.4 CURRICULUM VITAE

Name: Markus Kraller, BSc

Date of Birth: 20.09.1988

Place of Birth: Traunstein, Germany

Nationality: German

E-Mail: kraller-gessenhausen@t-online.de

Education

since September 2013   Master Thesis

                                                         Mechanism of Ras protein transfer from tumor
                                                         cells to endothelial cells

                                                         Group: Ao.Univ.-Prof.Dr. Christine Brostjan

                                                         Medical University, Vienna

October 2012 to October 2014   University of Vienna

                                                         Master studies in Molecular Biology

                                                         Focus on Biochemistry

October 2009 to May 2012   Paris Lodron University of Salzburg

                                                         Bachelor studies in Molecular Biology

                                                         Degree awarded: Bachelor of Science

                                                         Average grade: 1.7 (Austrian scale 1-5)

September 2008 to Mai 2009

Civilian Service

Hospital Traunstein

Intensive care unit

September 1999 to June 2008

Secondary school

Chiemgau Gymnasium Traunstein

Bavaria, Germany

Work experience

July 2013 to August 2013

Internship

Effects of radiofrequency electromagnetic fields on the yeast cells sterol metabolism, protein content and genome instability

Department of Physiology of Industrial Microorganisms; Zabolotny Institute of Microbiology and Virology Kiev, Ukrainian National Academy of Sciences

Supervisor: Prof. Dr. Elena Gromozova E.N.

Mai 2013 to June 2013

Internship

Production and purification of recombinant VP1 capsid protein from human rhinovirus type C

Department of Medical Biochemistry, Max F. Perutz Laboratories,

Supervisor: Prof. Dr. Heinrich Kowalski / Prof. Dr. Dieter Blaas

February 2013 to April 2013	Internship
	Deriving a single chain antibody fragment from the monoclonal antibody 2C11 as a monovalent tool to label CD3 subunits of the T cell receptor
	Medical University of Vienna: Center for Pathophysiology, Infectiology and Immunology (CePII), Institute for Hygiene and Applied Immunology
	Supervisor: Prof. Dr. Johannes Huppa
June 2012 to August 2012	Internship
	Investigation of potential beneficial effects of glutaraldehyde modified birch poll allergen in SIT
	Allergy Center Charité, Department of Dermatology, Venerology and Allergology, Berlin, Germany
	Supervisor: Prof. Dr. Margitta Worm
June 2011 to July 2011	Bachelor-Thesis
	Manipulating endogenous CRAC currents by STIM1 mutants Johannes Kepler University of Linz, Department of Physics,
	Institute of Biophysics: Ion Channel Group
	Supervisor: Prof. Dr. Christoph Romanin